J. E. Anthony

DOI: 10.1002/anie.200604045

Organic Electronics

The Larger Acenes: Versatile Organic Semiconductors

*John E. Anthony**

Keywords:
acenes · aromaticity · conducting materials · fused-ring systems · semiconductors

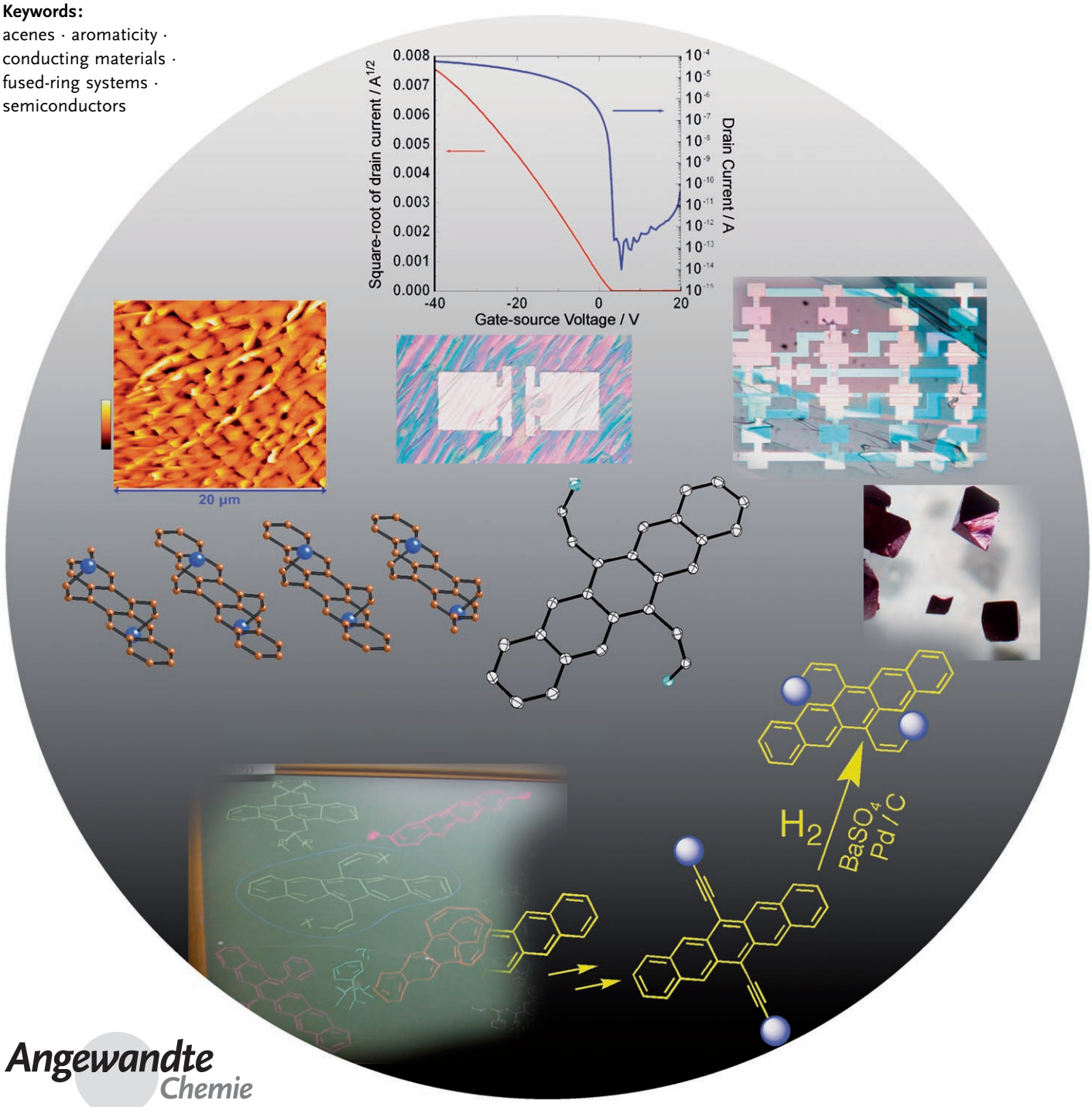

Acenes have long been the subject of intense study because of the unique electronic properties associated with their π-bond topology. Recent reports of impressive semiconductor properties of larger homologues have reinvigorated research in this field, leading to new methods for their synthesis, functionalization, and purification, as well as for fabricating organic electronic components. Studies performed on high-purity acene single crystals revealed their intrinsic electronic properties and provide useful benchmarks for thin film device research. New approaches to add functionality were developed to improve the processability of these materials in solution. These new functionalization strategies have recently allowed the synthesis of acenes larger than pentacene, which have hitherto been largely unavailable and poorly studied, as well as investigation of their associated structure/property relationships.

From the Contents

1. Introduction

Acenes have been the subject of intense study for well over a century. They are the most extended class of fused polycyclic hydrocarbons, typically described by the fewest localized Clar resonant sextets per number of aromatic rings.[1] Applications of these materials run the gamut from use as moth repellents to the starting materials for artificial dyes such as alizarin. More recently, these molecules have received attention for their electronic properties. One of the most appealing aspects of acenes in this respect is the rapid evolution of properties as oligomer length is increased—for example, an acene will have a smaller HOMO–LUMO gap than any other hydrocarbon with an identical number of aromatic rings. This same rapid evolution unfortunately also carries over to the stability of acenes—the largest well-characterized acene is only the five-ringed pentacene, and almost nothing is known about acenes larger than the six-ringed hexacene.

The small acenes naphthalene and anthracene are readily available because they are isolated from petroleum resources—anthracene, for example, from anthracene oil (the coal tar fraction distilling above 270 °C). These compounds can therefore be obtained on large scales,[2] and the intrinsic charge-transport properties of the ultrapure samples could be determined.[3] The detrimental effects of small levels of impurities on the charge-transport properties of organic solids could also be demonstrated unambiguously by adding impurities back into high-purity materials.[4] These landmark studies by Karl and co-workers demonstrated both the remarkable electronic properties inherent to acenes, along with the exceptional levels of purity required to exploit these properties.[5]

Acenes larger than anthracene are not isolated from petroleum deposits. The necessity of synthesis, along with the decreased stability and solubility, explains the 100-fold increase in cost for tetracene relative to anthracene, as well as the more limited quantities of materials typically available. Despite these drawbacks, larger acenes have come under intense scrutiny over the last decade as promising organic semiconductors because of their low-lying HOMO energy levels and strong two-dimensional electronic interactions in the solid state. A number of other important electronic properties also scale with the size of the acene, such as decreasing reorganization energy[6] and increasing carrier mobility[7] and band width.[8] Further, it has been predicted that the exciton binding energy decreases rapidly with increasing acene length, which bodes well for the use of larger acenes in photovoltaic applications.[9] Unfortunately, increasing acene length tends to also lead to significantly decreased stability.[10]

The credibility of acene research suffered a significant setback in 2002 when it was revealed that Hendrik Schön's data supporting many exceptional properties of these materials (solid-state injection lasers from tetracene,[11] superconductivity in anthracene, tetracene, and pentacene,[12] and hole mobilities in pentacene as high as 1200 $cm^2 V^{-1} s^{-1}$ [13]) had been fabricated. An investigation conducted by Bell Laboratories, Lucent Technologies,[14] led to the retraction of nearly all of these articles.[15] Although these false reports raised undue excitement in the field of organic electronics, and also wasted significant effort in a number of research groups attempting to reproduce or improve upon the results and materials described by Schön, the strength of the reliable publications involving the use of acenes in the field of organic electronics has helped maintain the viability of research in the use of acenes as organic semiconductors.

1.1. Organic Electronics

Efforts to synthesize, functionalize, and characterize larger acenes are driven by the potential to use these

[*] Prof. J. E. Anthony
Department of Chemistry
University of Kentucky
Lexington, KY 40506-0055 (USA)
Fax: (+1) 859-323-1069
E-mail: anthony@uky.edu

compounds in the field of organic electronics. The ability to replace inorganic semiconductors with organic counterparts will decrease manufacturing costs and allow fabrication of devices over large areas or on lightweight, flexible substrates. Soluble semiconducting organic "inks" can also be deposited and patterned by a variety of traditional printing techniques, such as ink-jet printing or screen printing,[16] further driving the development of soluble organic semiconductors. Many organic materials other than acenes can serve as the semiconducting layer in organic devices, and both polymeric[17] and small-molecule[18] semiconductor classes have been reviewed recently.

Acenes are at the forefront of efforts to find a versatile semiconductor for a number of lower-performance devices in which amorphous silicon is currently employed. Field-effect transistors are a major focus area, and these devices are being tailored for use in flat-panel displays and RFID tags (a possible replacement for the optical bar code).[19] The unique functionality of organic semiconductors is also being exploited for use in sensors.[20] The excellent hole (cation) transport properties of many organic semiconductors also make them suitable for use in photovoltaic devices. Organic solar cells will provide less expensive, lighter weight, flexible alternatives to traditional silicon-based devices: some organic solar cells based on conjugated polymers already exhibit efficiencies in excess of 4%,[21] which provides a benchmark for acene-based systems. Another use of acenes in display technology is as the emissive layer in OLEDs.[22] These devices aim to replace liquid crystals with emissive pixels for flat panel displays, and can consume less power than liquid-crystal systems, provide wider viewing angles, and lead to thinner, more flexible displays.

1.2. Charge Transport Measurements in Organic Solids

One of the most important characteristics to be determined for organic semiconductors is the charge carrier mobility (μ), which is a determining factor in the performance of organic electronic devices such as field-effect transistors, solar cells, and light-emitting diodes. This value, reported as $cm^2 V^{-1} s^{-1}$, is the drift velocity of the charge carrier (in $cm s^{-1}$) per unit electric field ($cm V^{-1}$). A number of methods can be applied to organic compounds to determine carrier mobility (in acenes, for which positively charged carriers predominate, hole mobility is of particular importance), including time-of-flight (TOF), space-charge-limited current (SCLC), and field-effect transistor (FET) measurements. However, other methods such as time-resolved microwave conductivity[23] and transient photoconductivity measurements[24] allow the extraction of mobility free of contact effects.

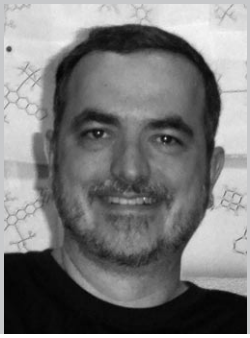

John Anthony received his B.A. in chemistry from Reed College and performed doctoral research with Prof. François Diederich at the University of California (UCLA) and at the ETH in Zürich. He returned to UCLA for postdoctoral studies with Prof. Yves Rubin. Since 1996 he has been in the Department of Chemistry at the University of Kentucky, where his research has been directed toward the synthesis of new organic semiconductors.

1.2.1. Time of Flight Measurements

Early benchmark measurements of carrier mobility in high-purity organic solids were performed by Karl and coworkers by using the TOF technique (Figure 1).[25] Although the technique conveniently yields a direct measurement of carrier mobility in the solid, there are a number of limitations. The crystal must be sufficiently thick relative to the penetration depth of the incident light beam to assure that carriers are only generated close to the transparent electrode. Further, the lifetime of the photogenerated carriers must be sufficiently long for them to traverse the space between electrodes, which means that typically only very thin crystals can be used, and they must be as free of defects as possible.

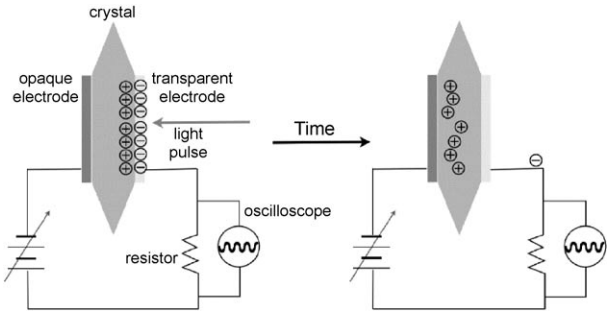

Figure 1. For a TOF experiment, the crystal is coated with two electrodes (one of which is semitransparent). A sheet of charge carriers is generated near the transparent electrode by an intense light pulse, and the voltage across the electrodes causes one type of charge carrier (in this case, holes) to migrate towards the nontransparent electrode. The arrival of the carriers at the electrode generates a current (displacement current). The velocity of the carriers (mobility) can be calculated from the duration of the current pulse and the thickness of the crystal. The width of the pulse also yields information on the number and nature of traps in the sample, which slow the progress of some proportion of the charge carriers.

Although there are numerous restrictions that must be met for a successful TOF experiment, there are also several advantages to this approach. Most importantly, because the charge carriers are generated by illumination and the resulting current is measured capacitively, the measurement is independent of electrode contact effects. This alone is of remarkable benefit, as high-quality electrical contact between organic solids and metal electrodes can be difficult to achieve. Further, measurements taken at different temperatures can be used to determine the concentration of shallow "traps"—defects in the solid that slightly stabilize charge carriers, impeding their movement through the crystal. A decrease in measured TOF mobility with decreasing temperature is a clear indication of the trapping and release of the charge carriers,[26] and this technique can be used to determine the relative energy (depth) of these traps.

1.2.2. Space-Charge-Limited Current

The least equipment-intensive approach to determine carrier mobility involves measurement of the current/voltage behavior at high electric fields to determine the mobility from the space-charge-limited current (Figure 2).[27] The setup

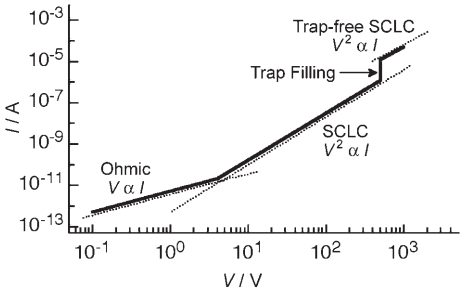

Figure 2. Carrier mobility can be extracted from the current/voltage behavior of a crystalline or thin-film sample. At low electric field, the behavior is ohmic. At higher fields, the injected charge concentration exceeds the equilibrium (before injection) charge concentration, leading to a space-charge-limited current (SCLC). In this regime, current is proportional to voltage squared ($I \propto V^2$). With increasing bias, all traps in the conduction pathway are eventually filled, leading to a dramatic increase in current (the trap filling regime). With a further slight increase in potential, the trap-free SCLC region is attained, from which accurate mobility determination can be performed.

typically involves the deposition of electrodes on opposite crystal surfaces (although coplanar electrode configurations can be used[28]), and determination of the current/voltage behavior through the four regimes described in Figure 2. Data from the trap-free SCLC region can be processed using Child's law,[29] or one of the more recent equations that account for trapping effects and field dependence issues,[30] to extract the charge carrier mobility (for details and caveats on this process, refer to a recent review article[52]). Information regarding the bulk electronic properties, including trap densities and trap distribution, can also be obtained: the displacement between the two SCLC regions indicates the energetic location of the traps in the band gap, and the voltage at which the trap-filling regime occurs yields the concentration of trapped states.[31]

Because carriers in the SCLC experiment are injected by the electrodes, a meaningful SCLC measurement can only be obtained when the contacts are ohmic (otherwise measured current will be injection-limited rather than space-charge-limited). Achieving an ohmic interface is complicated by the conditions required to form the electrode, because both the application of silver paint/epoxy or evaporation of metal electrodes can damage the organic surface, leading to deep interface traps.

1.2.3. Field-Effect Transistors

Field-effect transistors (FETs, Figure 3) are a versatile platform for the study of organic semiconductors. Transistor characteristics reveal information regarding carrier mobility, the quality of the electrode and substrate interfaces, and the

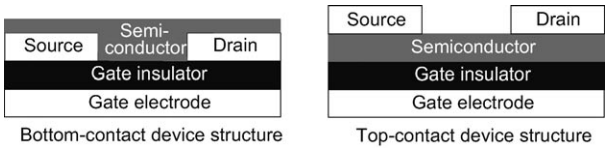

Figure 3. Field-effect transistors can be fabricated in two configurations: bottom-contact (left) and top-contact (right). The source and drain electrodes are in contact with the organic semiconductor and separated from the gate electrode by an insulator with a high dielectric constant. With no gate-source bias, very little current flows between source and drain electrodes, and the transistor is in the "off" state. Application of gate-source voltage causes charging at the dielectric surface and induces charge in the semiconducting layer (similar to the charging of a capacitor). The increased number of charge carriers in the channel yields a significant increase in conductivity in the sample, turning it to the "on" state. Gate-dependent conductivity can be used to extract the carrier mobility.

purity of the organic sample. Further, because FETs are also a major component of flat-panel displays, the development of improved methods to study organic transistors will also inform fabrication processes for commercial applications of these materials. The charge carrier mobility is extracted from the transistor performance by Equation (1).

$$I_{DS} = \frac{W C_i}{2 L} \mu (V_G - V_0)^2 \quad (1)$$

I_{DS} is the current measured between source and drain electrodes, W is the channel width (the gap between source and drain electrodes), L is the channel length (the distance between source and drain electrodes), μ is the field-effect mobility, V_G is the applied gate voltage, V_0 is the threshold voltage, and C_i is the capacitance of the gate insulator. A plot of the square root of the drain-source current versus gate voltage yields the square root of $(\mu W C_i/(2L))$, from which the mobility is easily extracted. To be competitive with amorphous Si devices, organic transistors must exhibit mobility μ greater than 0.5 $cm^2 V^{-1} s^{-1}$, and an on/off current ratio ($I_{on/off}$, the ratio of the drain–source current in the on and off states) greater than 10^5. Further, from a practical standpoint the threshold voltage V_{th} (the voltage at which carriers accumulate between source and drain electrodes and the transistor begins to turn to the "on" state) should be zero or slightly negative, so that in the absence of gate bias the device is truly in its "off" state.[32]

2. Scope

A recent review of acenes covered the history of acenes, their synthesis, early characterization, and detailed analyses of the theoretical studies performed to elucidate the reactivity, as well as the nature of aromaticity in this class of compounds.[33] A recent review of functionalized acenes and heteroacenes covered the use of these compounds in electronic devices,[34] and the structural aspects that yield improved device performance. Herein we will focus instead on acenes larger than anthracene, particularly the parent

hydrocarbons (tetracene and pentacene), and studies of their electronic and device properties. Particular emphasis will be placed on recent single-crystal studies that have helped to elucidate the intrinsic transport properties of these compounds, and on the optimization of device fabrication techniques to improve performance. We will present the most recent functionalization strategies to impart solubility, stability, or improved ordering to the materials. Because nonlinear benzannelation has been shown to degrade the electronic properties of acenes dramatically, this class of materials will not be covered.[35]

3. Tetracene

Tetracene (**1**) is a bright orange crystalline material that sublimes readily above 170 °C.[36] Its oxidation potential is 720 mV (vs. SCE) and longest wavelength absorption maximum is at 474 nm.[37] The material crystallizes in the triclinic $P\bar{1}$ space group with two molecules in the unit cell and an edge-to-face "herringbone" arrangement characteristic of acenes.[38] Although **1** is not isolated from natural petroleum distillates or coal tar, it can be produced by the combustion of organic products and has been found in diesel exhaust[39] and on char-grilled beef.[40] **1** was the first reported photochromic molecule; in solution, **1** can be photodimerized to yield colorless "butterfly compound" **2**, which upon heating reverts to **1** (Scheme 1).[41] **1** has also been used in the formation of

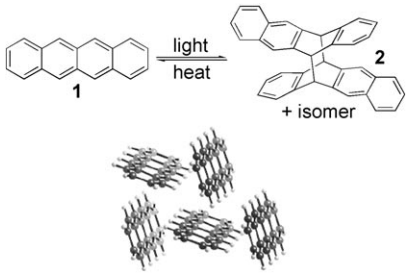

Scheme 1. Reversible photodimerization of tetracene, and tetracene crystal packing.

some fascinating organometallic sandwich compounds,[42] and as a dopant for the construction of carbon-nanotube-based devices.[43] Several studies have been performed to understand the nature of phase transitions in **1** and their effect on the electronic properties of single crystals. In pressure-dependent studies, the photoconductivity of **1** was found to increase rapidly as pressure was applied, likely as a result of the decrease in the separation between molecules in the crystal and concomitant increase in the intermolecular transfer integral.[44] This rationale is also supported by the red shift in optical absorption observed for some acenes when the crystals are placed under pressure.[45] Detailed studies of changes in phonon modes as a function of pressure in these systems have also been performed.[46] A dramatic decrease in the photoconductivity of **1** starting at an applied pressure of 0.3 GPa was shown to correspond with a pressure-induced phase transition,[47] which has also been observed by Raman spectroscopy and was further shown to occur in samples that were cooled below 140 K. The low-temperature (or high-pressure) phase of **1** is predicted to involve a denser packing than seen in the room-temperature form, which makes it of significant interest for device utilization. The transition to this low-temperature phase also explains the difficulty in obtaining single-crystal FET mobility measurements at extremely low temperatures.[48]

3.1. Tetracene and Rubrene Single-Crystal Studies

Perhaps the most significant recent advances in the understanding of the intrinsic electronic properties of organic materials has arisen with the development of efficient methods to grow large, high-quality single crystals of tetracene (**1**) and 5,6,11,12-tetraphenyltetracene (rubrene (**3**), Figure 4), allowing the fabrication of semiconductor devices

Figure 4. Rubrene (**3**) and its crystal packing (CSD code: QQQCIG).

directly on their surfaces.[49] A key aspect in the performance of these devices is the purity of the organic material,[50] which must be cleaned by sublimation before the process of crystal growth can begin. Access to high-purity crystals allows the measurement of electronic properties in a nearly homogeneous sample that is relatively free of impurities and defects such as crystalline grain boundaries.

Both **1** and **3** form high-quality crystals by physical vapor transport, whereby the purified acene is heated under constant flow of a carrier gas in a tube to which is applied a shallow temperature gradient.[51] The optimal crystal-growth methods, particularly the temperature gradient, must be determined for each material. Also, because the process is not carried out under vacuum, high temperatures are required, which necessitates that the organic materials be thermally stable. The nature of the carrier gas has also been found to be critical to the formation of high-quality crystals.[52]

3.1.1. TOF Studies

Time of flight measurements have been performed on high-quality crystals of tetracene purified by gradient sublimation. The measured hole mobility was highly consistent across a range of samples with a typical value of 0.69 $cm^2 V^{-1} s^{-1}$ at 330 K. Although this value is less than that reported for transistor measurements of single crystals (see Section 3.1.3), it is important to consider the geometry of the measurement. TOF measurements of platelike acene

crystals typically determine the mobility along the crystallographic axis with the least amount of electronic interactions (the direction of strong intermolecular interaction typically lies on the crystallographic *ab* plane, which is the plane probed by transistor measurements).[53] The authors also performed a detailed analysis of the impurities present in tetracene samples and found that the major contaminant was 5,12-tetracenequinone. Because of the electron-deficient nature of this impurity, it likely serves an electron trap, and the presence of such impurities in acene samples may be responsible for their low electron mobilities.[54] The results of these experiments underscore the problems associated with the presence of small impurities in organic semiconductor samples and the need to develop efficient methods to purify these aromatic species.[55]

3.1.2. SCLC Studies

Both **1** and **3** have proven amenable to SCLC studies. Recent analyses of crystals of **1** by this method yielded surprisingly inconsistent results: the mobilities derived from SCLC measurements for a batch of very similar crystals vary over several orders of magnitude.[56] Much of this variation arises from defects at the crystal surface, caused by slightly different conditions for crystal growth (even for crystals grown together in the same sublimation apparatus) or by varying amounts of damage from the deposition of the electrodes.[57] The SCLC for crystals of **1** is only weakly temperature dependent, implying the limiting factors are injection phenomena, not carrier transport issues.[58] Nevertheless, some samples of **1** have been prepared with electrode contacts sufficiently good to observe the necessary trap-free SCLC regime,[56] yielding hole mobility as high as $1\ cm^2 V^{-1} s^{-1}$. Samples in this study with mobilities greater than $0.1\ cm^2 V^{-1} s^{-1}$ generally exhibited an increase in hole mobility as temperature was lowered, but it decreased abruptly at 180 K owing to the phase transition.[59] Studies on high-quality crystals of **3** also yield excellent data in SCLC experiments. Recent results using silver electrodes deposited onto the surface of **3** through a collimator yielded high-quality contacts, as evidenced by the observation that the resistance across the metal/organic contact was significantly less than that across the organic crystal being measured.[60] All four regions described in Figure 2 were observed in the *I*/*V* graph for this device, with the SCLC regime beginning at a bias of only 2.5 V. In this case, the authors did not calculate the carrier mobility, but they did determine that the trap density in the crystal was approximately $10^{15}\ cm^{-3}$.

A comparison of hole mobility in single-crystals of **1** determined by both SCLC and TOF methods showed that these methods can produce similar results ($\mu \approx 1\ cm^2 V^{-1} s^{-1}$), and that both methods show increasing mobility with decreasing temperature. Comparisons of measured values from these two methods can provide detailed information about the nature of charge traps in the crystal. For example, TOF measurements place the depth of relatively shallow traps (likely dislocations or deformations of the crystal lattice) at about 100 meV, whereas the most significant defects (deep traps) likely arise from damage caused by the attachment of electrodes to the crystal surface. In contrast, both the density and the depth of deep traps can be extracted from the SCLC curves, in this case yielding values of $5 \times 10^{13}\ cm^{-3}$ and 700 meV, respectively.[56]

3.1.3. FET studies

To determine the intrinsic electronic properties of organic materials by using transistor devices requires access to large crystals with smooth surfaces,[51] and great care must be exercised during device fabrication to avoid damaging the crystal surface. The first-generation single-crystal organic FETs were constructed by traditional fabrication procedures with conditions and materials designed to minimize the damage to the organic surface. Vacuum deposition of a highly collimated beam of silver, deposited at a very slow rate from an evaporation boat held 70 cm from the crystal surface, proved suitable for the formation of the source and drain electrodes with minimal damage to the crystal surface.[61] Deposition of the gate dielectric similarly required great care, and it was discovered that insulators typically used for TFTs (SiO_2, Al_2O_3) cannot be deposited safely on organic crystals. In this case, the organic dielectric polymer parylene, which can be thermally deposited, was used to form the necessary insulating layer.[60] This polymer is generated by thermal decomposition of the aromatic cyclophane *p*-xylylene under vacuum at around 700 °C in a pyrolysis tube, the output of which is directed at the organic sample (Figure 5).

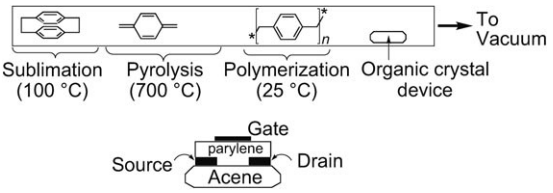

Figure 5. Apparatus for deposition of parylene, and a single-crystal FET.

Alternative approaches to single-crystal device fabrication entirely circumvent issues with damaging the organic crystal surface by fabricating the components of the transistor device on a rigid or flexible substrate, and then electrostatically bonding or laminating the crystal onto the surface of the device. Electrostatic bonding requires an exceptionally clean device surface containing polar, reactive functional groups, which can be achieved by treatment of the device with oxygen plasma.[62] When the transistor device is fabricated on a flexible poly(dimethylsiloxane) (PDMS) stamp, the crystal can be completely laminated onto the device by light pressure on the flexible substrate. A further advantage of the PDMS stamp devices is the reversibility of the lamination process, which allows repeated measurement of the crystal.

3.1.3.1. FETs with Tetracene Single Crystals

Early studies with tetracene single-crystal transistors used a FET configuration on a heavily doped Si wafer, which

required very thin crystals (< 1 μm) that were able to conform to the patterned device (Figure 6).[62a] These devices showed hole mobility on the order of 0.4 $cm^2V^{-1}s^{-1}$ and an unusual temperature dependence; the measured mobility increased with decreasing temperature in the range 330–270 K, then decreased again in the region 270–220 K. This phenomenon likely arises from the presence of shallow traps, which only become a significant impediment to charge transport at relatively low temperatures.

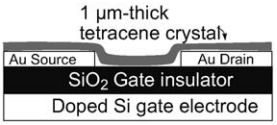

Figure 6. Lamination of a tetracene crystal onto a surface to produce a traditional bottom-contact FET structure.

Several approaches to improving the contact interface in laminated tetracene single-crystal FETs have been reported.[53] Because this technique involves electrostatic bonding of the crystal to the device (fabricated on a silicon wafer/SiO_2 layer, Figure 6), it was hypothesized that treatments of both the dielectric surface and the source/drain electrodes could be employed to improve adhesion or electronic contact. First, the SiO_2 dielectric was treated with octadecyltrichlorosilane to minimize the number of charge carriers trapped at the interface between the hydrophobic crystal and the polar gate insulator.[63] Second, the gold electrodes are treated with 4-trifluoromethylbenzenethiol, an electron-deficient aromatic species that will interact strongly with the electron-rich acene crystal to improve charge injection and decrease contact resistance between the crystal and the electrodes. These treatments improved device reliability and reproducibility, providing single-crystal devices of **1**, **3**, and pentacene with mobilities of 1.3, 10.7, and 1.4 $cm^2V^{-1}s^{-1}$, respectively. The nature of the dielectric treatment also has a significant impact on threshold voltage, which is shifted over a range of 30 V by selection of the appropriate monolayer.[64] A similar approach to dielectric functionalization was used in the preparation of vapor-deposited pentacene FETs.[65]

The use of a polymer electrolyte as gate dielectric in **1** and **3** single-crystal FETs led to extremely high carrier density upon application of gate voltage ($> 10^{15}$ charges cm^{-2}), which oxidized essentially all of the molecules at the dielectric interface. The presence of such a high number of carriers allowed modulation of the drain current over 5 orders of magnitude within a range of 3 V—an impressive sensitivity for organic semiconductors.[66]

3.1.3.2. FETs with Rubrene Single Crystals

Rubrene is one of the most highly studied materials in single-crystal transistor research because of its ready availability and ease of crystal growth. The aryl substituents on the most-reactive acene rings hinder the oxidative decomposition so that no quinone decomposition product is formed. However, **3** is not immune to decomposition. In a recent study of the crystal growth of **3**, two impurities were isolated in this material.[67] Compound **4** was found both after crystal growth and in samples of the as-purchased **3**, and may be a by-

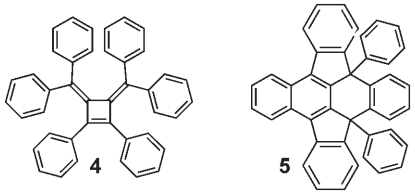

product of the synthesis process. Compound **5**, in contrast, was likely formed by a thermal oxidative process during the crystal-growth procedure. The structures of these two impurities were determined crystallographically, and it was possible to form working single-crystal FETs on the surface of crystals of **4**. The mobility determined for this compound was 0.02 $cm^2V^{-1}s^{-1}$, which is significantly lower than that found for **3**.

The earliest attempts at forming transistors on free-standing single crystals of **3** used thermally evaporated silver source and drain electrodes and parylene gate insulator to yield devices with mobilities ranging from 0.1 to 1.0 $cm^2V^{-1}s^{-1}$.[60] Further optimization of device fabrication led to an increase in measured mobility to 8 $cm^2V^{-1}s^{-1}$.[61] The high hole mobilities measured in single crystals of **3** triggered detailed and elegant ab initio computational studies, which showed that the particular π-stacking of the aromatic rings of adjacent molecules of **3** led to significant overlap of areas of high HOMO density (Figure 7).[68] The minimal short-axis slip of the interacting molecules of **3** is also key to the high measured mobility.

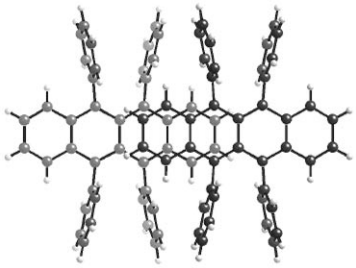

Figure 7. π stacking in a pair of rubrene molecules. Unlike most π-stacked acenes, there is no short-axis slip in the stacking.

High-quality single crystals of **3** were studied in FET configurations by using source and drain electrodes patterned on a flexible PDMS stamp as well as air (or vacuum) gap configurations (Figure 8) designed to eliminate surface interactions with the portion of **3** in the active device channel.[69] Removal of gate–insulator contact issues led to a significant increase in hole mobility (up to 20 $cm^2V^{-1}s^{-1}$ at 300 K) along with the realization of significant mobility anisotropy and

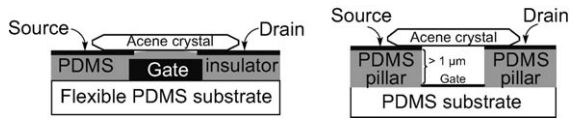

Figure 8. Acene crystal transistors using a flexible PDMS substrate (left) or a vacuum gap/air as gate dielectric (right).

increasing mobility down to 150 K. At that temperature, the mobility began to drop exponentially, and the mobility anisotropy observed at higher temperatures disappears. The existence of several potential polymorphs for **3**[70] raises the possibility that this change in behavior is due to a phase transition in the solid. This possibility was investigated crystallographically to determine whether there were any changes in structure across the temperature range from 100 to 300 K—none were found.[71] A reasonable explanation for these changes in mobility involves charge-carrier traps (with depth < 70 meV), which at sufficiently low temperature cause the carrier transport to shift to a multiple trap and release mode, thus decreasing mobility.

Fabrication of transistors on flexible PDMS stamps allows the removal and replacement of crystals of **3** without degradation of electronic properties, thus permitting more detailed exploration of the charge transport properties.[72] Simple rotation of the crystal on the device along an axis parallel to the crystallographic *c* axis allowed the measurement of the hole mobility across a large sampling of molecular orientations in the crystallographic *ab* plane. Mobility was highest along the molecular π-stacking axis and lowest perpendicular to this axis (where interactions are predominantly edge-to-face). The mobility relative to molecular orientation is shown in Figure 9.

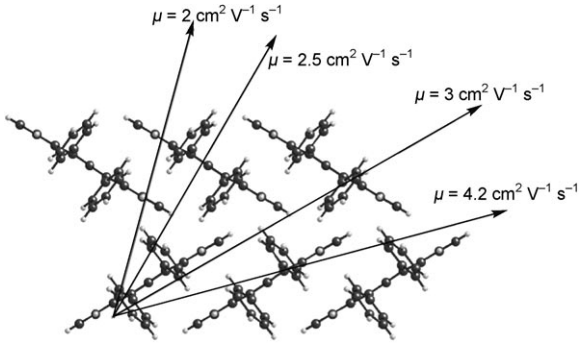

Figure 9. Mobility in single crystals of rubrene (**3**) as a function of source–drain electrode orientation (adapted from reference [72]).

Recent evidence for bandlike (rather than hopping) transport of charges across the surface of high-purity organic systems has been provided by the observation of the Hall effect in FETs fabricated on crystals of **3**. The Hall effect, which describes variations in electronic properties as a function of applied magnetic field, can be used to determine the charge-carrier density, resistivity, and intrinsic mobility of a sample, as well as the sign of the dominant charge carrier. In this case, the probes used to measure the Hall voltage are inserted between the source and drain electrodes of the transistor to measure these values in the channel region of the device. Vacuum-gap, parylene, and SiO_2 insulator devices have been used for these studies (Figure 10). The applied gate

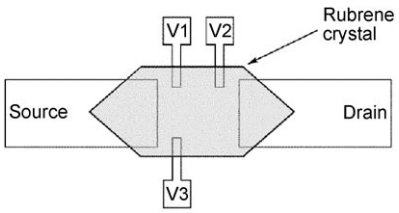

Figure 10. Configuration of electrodes on the gate insulator surface for measurement of the Hall effect in single crystals of **3**.

voltage ensures a sufficient population of carriers to generate a delocalized electron cloud at the surface of the crystal, and the source–drain voltage is kept constant (e.g. at 5 V). The Hall voltage (V_H) can be measured either along the channel (V1–V2)[73] or across the channel (V1–V3),[74] as a function of variation in magnetic field (0–10 T) applied perpendicular to the sample. The number of free (i.e. unencumbered by trap states) carriers and the Hall mobility can be easily calculated from the dependence of V_H on applied field. For **3**, the density of carriers derived from the Hall measurement matches well the carrier density expected on the basis of the capacitance of the dielectric and applied gate voltage. More importantly, the measured increase in Hall mobility with decreasing temperature supports the assignment of diffusive transport of charge carriers through large, many-molecule delocalized states between trapping sites.

Ambipolar (both hole and electron) transport has also been observed recently in single crystals of **3**.[75] Ambipolar transport is an unusual phenomenon in acene systems, as these arenes are typically more easily oxidized than reduced, which makes injection of holes much easier than injection of electrons. One method to check for n-type (electron as the dominant carrier) behavior in simple aromatic compounds such as **3** is to exploit low work function electrodes, which enhance the ability of the electrodes to inject electrons into the LUMO of the organic crystal. An additional complicating issue is the high reactivity of aromatic anions—these species typically react rapidly with hydroxy groups on the surface, as found in common gate dielectric materials such as SiO_2. Because the active region of organic transistors consists of only the first few monolayers of material at the dielectric surface in the active channel,[76] reactions at this surface will quickly quench charge transport. Thus, single-crystal FET devices of **3** formed with Ag electrodes and a PMMA gate dielectric free of hydroxy groups yielded well-defined transistor characteristics in both p-channel and n-channel current modes. As is common in acene semiconductors, the hole mobility ($1.8\ cm^2V^{-1}s^{-1}$) was significantly higher than the electron mobility ($0.011\ cm^2V^{-1}s^{-1}$).

3.2. Tetracene Thin-Film Devices

In the earliest applications of thermally evaporated thin films of **1** in transistor devices no field effect was observed.[77] A decade later, fabrication methods leading to highly ordered thin films of **1** yielded transistors with reasonable performance. Treatment of the SiO_2 gate dielectric with octadecyltrichlorosilane (OTS) to yield a highly ordered, hydrophobic monolayer prior to deposition of **1** was found to improve crystalline order in the thermally evaporated films dramatically.[78] The hole mobilities in these FETs were higher than 0.1 $cm^2 V^{-1} s^{-1}$ with excellent on/off current ratios (10^7). AFM studies of the films of **1** revealed decreased nucleation density on OTS-treated substrates, which led to improved film ordering and grain interconnection as a result of the higher surface mobility of initial molecules deposited on the treated substrate. This treatment can also yield a significant increase in connectivity in the portions of the film that are in direct contact with the treated substrate.[79]

3.2.1. Tetracene in Solar Cells

Tetracene is an appealing material for photovoltaic studies because of its relatively good oxidative stability, good absorption and fluorescence properties, and high measured hole mobility. A significant barrier to the adoption of soluble derivatives of **1** (or pentacene) in organic solar cells is their rapid [4+2] Diels–Alder reaction with fullerenes (commonly used as n-type materials).[80] One approach to mitigate this issue is the covalent linking of a soluble fullerene to **1** to form the highly soluble donor–acceptor dyad **6**

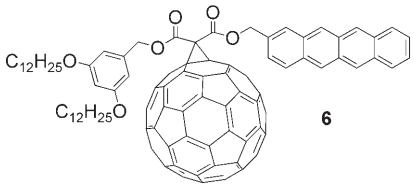

6

(Figure 11).[81] Photophysical studies showed that the normally strong fluorescence of **1** was completely quenched by the attached fullerene.

The issue of Diels–Alder reaction between fullerene and acene is not as relevant to materials deposited by thermal evaporation, whereby discrete layers of p- and n-type material are deposited sequentially to yield a single-heterojunction device. The Yang group recently reported the fabrication of **1**/C_{60} solar cells with external power conversion efficiencies as high as 2.3 %.[82] The key to the efficiency of this device was the high crystalline order of the 80-nm-thick layer of **1** (Figure 11). The device yielded a short-circuit current density of 7 $mA cm^{-2}$ and an open-circuit voltage of 580 mV under AM 1.5 (100 $mW cm^{-2}$) illumination (AM = air mass). The high open-circuit voltage is likely the result of the high HOMO energy level of **1** (relative to pentacene, which yields higher current but an open-circuit voltage of only 363 mV[262]).

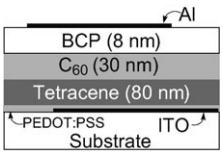

Figure 11. Structure of a tetracene-based solar cell. BCP = bathocuproine; ITO = indium tin oxide; PEDOT = poly(ethylenedioxythiophene); PSS = poly(styrenesulfonate).

3.2.2. Light-Emitting FETs

The high hole mobility of **1**, combined with its high fluorescence quantum yield, made it an excellent choice of material for the first investigation of electroluminescence in a FET configuration.[83] Because the major use envisioned for organic FETs is in the control of OLED pixels in flat-panel displays, light-emitting FETs (LEFETs) would constitute the highest degree of miniaturization and simplification for display applications. The earliest reported light-emitting transistor was fabricated with interdigitated gold source and drain electrodes (Figure 12) spaced 5 μm apart. The transistor

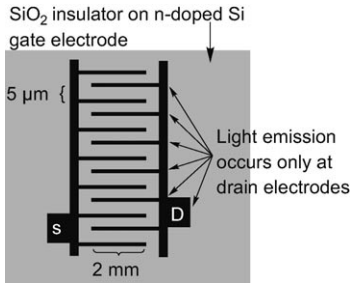

Figure 12. Device configuration for LEFETs. D = drain; S = source.

parameters for this device were reasonably good: $\mu = 0.05$ $cm^2 V^{-1} s^{-1}$, $I_{on/off} = 10^6$, and the semiconductor behaved as a p-type material. However, at higher voltages ($V_{DS} > -20$ V), emission of light from the layer of **1** was observed, implying the injection of electrons necessary for charge recombination and electroluminescence. Although the intensity of the light was not high (maximum 44 $cd m^{-2}$ at $V_{DS} = V_{GS} = -80$ V), this result is both an impressive demonstration of the potential of organic electronics, as well as an intriguing conundrum regarding the behavior of FETs at high voltages. How are electrons injected into the organic layer under these conditions? The authors of this early report observed that emission only occurred adjacent to the drain electrode and postulated that poorly mobile holes located far from the gate dielectric might migrate to the drain electrode to build a significant electric field at this location. Electrons would then be injected by field emission.

3.3. Functionalized Tetracenes

Acene functionalization can be used to tune a variety of important properties, such as solubility, stability, and phase behavior. A straightforward functionalization strategy involves the addition of π-conjugated substituents to alter the emission profile of the material. As their fluorescence quantum yields are also relatively high (ca. 20 %),[84] such materials can be used in light-emitting devices: rubrene (**3**)

has been used as a dopant in polyfluorene-based OLEDs to yield white emission,[85] and other tetracene derivatives have been studied as components of red-emitting OLEDs.[86] *Peri*-functionalized dialkoxy tetracenes such as **7** were used to

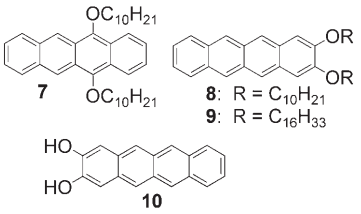

study the photodimerization of soluble acenes,[87] whereas the end-functionalized tetracenes **8** and **9** were investigated for their ability to form stable gels;[88] a similar pentacene derivative was also reported.[89] In contrast, the dihydroxy derivative **10** was used to form well-defined monolayers of this organic semiconductor on oxide surfaces.[90]

Several approaches to induce π-stacking interactions in tetracenes have been reported. Bao and co-workers used halogen groups to disrupt edge-to-face interactions in **1** to yield increased π-stacking interactions (Figure 13).[91] In this

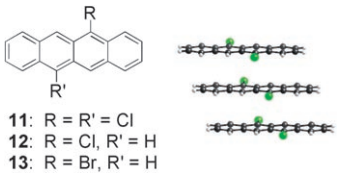

Figure 13. Structure and crystal packing of halotetracenes.

study, only the dichloro derivative **11** packed with extensive, long-range π-overlap to yield single-crystal FETs with hole mobility ($1.6\ cm^2V^{-1}s^{-1}$). The 1D π-stacking arrangement, however, did not translate to high performance in thin-film devices; the highest observed mobility was less than $0.001\ cm^2V^{-1}s^{-1}$.

Dipolar interactions have also been exploited to induce π-stacking of **1** in the solid state. The Swager group used partially fluorinated derivatives of **1** substituted with alkyl and alkoxy groups to yield soluble materials with significant π-stacking interactions in the crystal (Figure 14, left),[92] whereas the Nuckolls group obtained the crystal structure

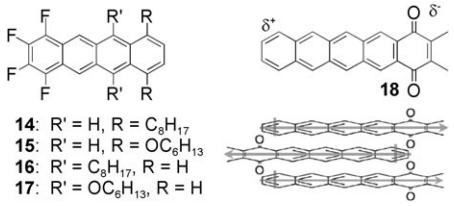

Figure 14. Left: Tetrafluorotetracenes **14**–**17**. Right: Dipolar interactions yield columnar π stacks in pentacenequinone **18**.

of 1,4-pentacenequinone **18**, which showed a π-stacked arrangement in the solid state (Figure 14, right).[93] Thin-film transistors fabricated from the corresponding 1,4-hexacenequinone exhibited a hole mobility of $0.05\ cm^2V^{-1}s^{-1}$.

Bitetracenes **19**–**21** have been prepared recently. Compound **19** showed remarkable photophysical properties,[94] whereas **20** and **21** both yielded highly stable transistor devices[95] with hole mobilities as high as $0.5\ cm^2V^{-1}s^{-1}$.

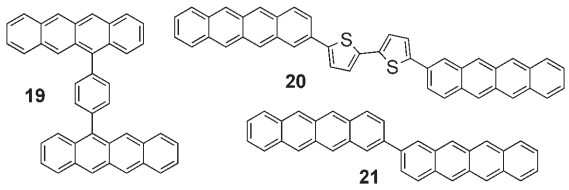

Although **3** has exhibited superior performance in single-crystal devices, films of **3** are generally not sufficiently uniform to produce high-performance thin-film devices.[96] Two recent approaches have begun to overcome the problems associated with thin films of **3**. The first involves blending **3** with an insulating polymer and subsequent thermal annealing to yield uniform films.[97] The second involves patterning the substrate to induce crystal nucleation of **3** during film growth.[98] Both approaches yield arrays of transistor devices with high hole mobility.

4. Pentacene

Pentacene (**22**) is a deep blue crystalline material that is only sparingly soluble in organic solvents, producing bright pink solutions owing to its intense red fluorescence—the longest wavelength absorption for this chromophore is 578 nm,[99] and it emits with a fluorescence quantum yield of around 8% (in cyclohexane[100]) at 585 nm.[101] The unique photophysical properties of **22** have been studied extensively by single-molecule spectroscopy[102] and in inert organic matrices.[103]

The crystal structure of **22** was first reported in 1961[104] but was revised in 1962.[105] Like **3**, **22** crystallizes in the triclinic $P\bar{1}$ space group with two molecules per unit cell and unit-cell dimensions $a = 7.90$, $b = 6.06$, $c = 16.01$ Å, $\alpha = 101.9$, $\beta = 112.6$, $\gamma = 85.8°$. Unlike smaller acenes, **22** adopts a number of polymorphic forms, and most modern studies of the single-crystal structure report slightly different unit-cell dimensions ($a = 6.275$, $b = 7.714$, $c = 14.442$ Å, $\alpha = 76.752$, $\beta = 88.011$, $\gamma = 84.524°$;[106] Figure 15). Calculations showed that these two phases occupy the two deepest potential minima for herringbone arrangements of **22** in the crystal.[107] There is some evidence that the earlier reported phase exists as a phase impurity in the more recently reported phase and that the crystal can transform entirely into the latter phase under pressure.[108]

Like **1**, **22** is not isolated from petroleum sources. It is formed in the combustion of carbon-rich polymers[109] and has been detected in the interior of meteorites.[110] It is most

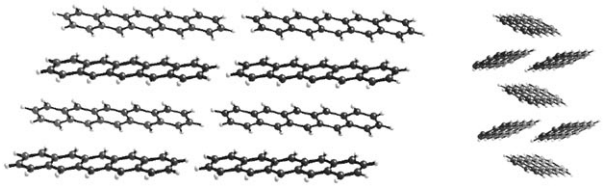

Figure 15. Layered herringbone packing of pentacene (**22**).

conveniently synthesized from 6,13-pentacenequinone (**25**), which is itself easily prepared by fourfold aldol condensation between phthalaldehyde and 1,4-cyclohexanedione.[111] **22** is then formed from **25** by a simple reduction reaction (Scheme 2).[112] Pentacene is significantly less soluble and

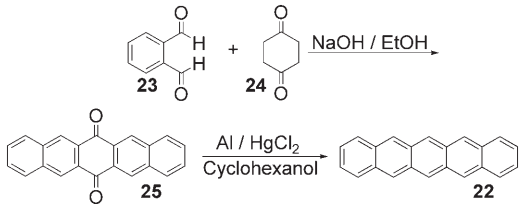

Scheme 2. Synthesis of pentacene from pentacenequinone.

less stable in solution than tetracene: very dilute solutions of **22** in 1,2-dichlorobenzene, for example, bleach within 5 minutes unless carefully isolated from both air and light.[113] However, provided air and light are excluded, solutions of **22** in hot 1,2,4-trichlorobenzene can be made sufficiently concentrated for the solution-based fabrication of transistors with reasonable performance parameters ($\mu = 0.45\ cm^2 V^{-1} s^{-1}$).[114] The main oxidative by-product of the decomposition of **22** is 6,13-pentacenequinone (**25**), which recent theoretical investigations have shown can be formed by reaction between **22** and either singlet oxygen in a concerted fashion, or with triplet oxygen by a stepwise, radical mechanism.[115] The resulting endoperoxide then converts quickly into **25**.

Solutions of **22** can decompose even in the absence of oxygen to yield the "butterfly dimer" **26** as a photodecomposition product. In contrast to the dimerization of **1**, the formation of this dimer is not easily reversible. Dimer **26** could be synthesized preparatively by irradiating a solution of

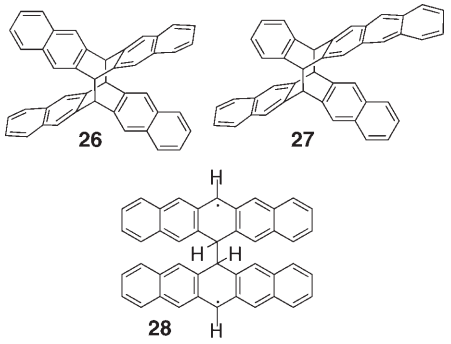

22 ($\lambda > 440$ nm) at 120 °C in deoxygenated 1-chloronaphthalene; dimer **26** precipitated as a white solid over the course of several days.[116] Photodimerization also yielded the asymmetric dimer **27** as a minor product. X-ray crystallographic analysis of **26** showed that the bonds connecting the two pentacene moieties are very long (1.58 Å). Although the dimer was thermally stable, it could be converted into **22** by UV irradiation for around 30 minutes. This photolysis was shown to proceed through a "broken dimer" intermediate (**28**), which could be trapped by photolysis of **26** in a PMMA matrix.

Pentacene also serves as a highly efficient diene in Diels–Alder reactions. The reaction between C_{60} and **22** is rapid in solution, typically forming 1:1 adduct **29** (Scheme 3). When the reactive 6,13-positions of pentacene are functionalized, Diels–Alder reactions still take place on the rings adjacent to the central ring—in the case of fullerene dienophiles, the bisadduct **30** has been isolated and studied crystallographically.[117]

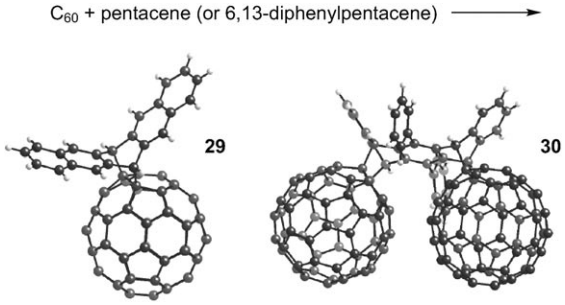

Scheme 3. Pentacene/fullerene adducts.

The stability of pentacene films and devices towards X-ray irradiation has also been determined to evaluate their suitability for use in space-based applications.[118] Exposure of pentacene-based thin-film transistors to intense radiation led to only a 14% decrease in transistor performance. The authors considered this result as evidence that pentacene-based transistors are intrinsically stable towards radiation damage.

4.1. Theory of Charge Transport in Pentacene

Long before **22** was first used in transistors, TOF experiments led researchers to speculate that charge transport in microcrystalline films of this molecule could occur by a dispersive mechanism.[119] Subsequent high mobilities determined by transistor measurement are buttressed by detailed theoretical investigations into the nature of efficient charge transport in **22**. Intermediate neglect of differential overlap (INDO) calculations based on the crystal structure of **22** predict significant bandwidths (608 meV for the valence band, 588 meV for the conduction band), which signify high intrinsic mobility.[120] The similar magnitudes of dispersion in the two bands implies that electron mobility in crystals of **22** should be as high as the hole mobility. A further factor

contributing to high carrier mobility in **22** is its low vibrational reorganization energy, a term that quantifies the energy required for a molecule to relax geometrically upon oxidation. A reorganization energy for **22** of 0.059 eV was found experimentally,[121] and a value of 0.098 eV was extracted from quantum chemical calculations.

Monte-Carlo studies on a number of parameters that could affect carrier mobility were carried out using a 1D stack of molecules of **22** as a model.[122] These studies supported earlier work that showed the amount of intermolecular overlap was not as important as the nature of that overlap; the strong interaction between HOMO orbitals on adjacent molecules was more important than simple overlap of the aromatic rings.[123] Band-structure calculations on the four thin-film polymorphs of **22** found significant differences in dispersion in the valence bands between these polymorphs.[124] Only one of the polymorphs (the 15.4-Å phase) showed significant dispersion throughout the crystallographic *ab* plane. Calculations incorporating the thermal motions of the pentacene molecule in the crystal showed that the fluctuations in intermolecular transfer integrals was of the same order of magnitude as the average values calculated from the "rigid" crystal.[125] Thus, at temperatures even as low as 100 K the crystal was considered to be disordered, and the band-transport model was deemed to be unsuitable for a complete description of transport in **22**.

4.2. Doped Pentacene

Changes in both structural and electrical properties were observed when vacuum-deposited films of **22** were doped with iodine.[126] The conductivity increased to 110 $S\,cm^{-1}$ (a factor of 10^{11} increase from undoped film), and X-ray diffraction analysis showed a significant change in the spacing of the pentacene layers, which implies localization of dopant anions (Figure 16). More detailed analyses showed that there were two attainable doping levels: the lower-level doping leads to I_3^- ions inserted between layers of **22**, whereas higher doping levels lead to I_5^- inserted within the layers of **22**, significantly expanding the crystal lattice.[127]

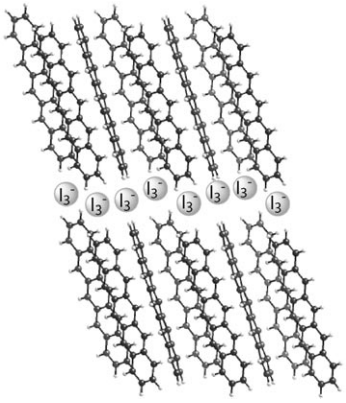

Figure 16. Intercalation of iodine dopant (as I_3^-) between pentacene layers.

Pentacene has also been n-doped with alkali metals to give similarly conductive complexes.[128] The conductivity of Li-doped samples at a **22**/Li ratio of approximately 1:1 was $6 \times 10^{-3}\,S\,cm^{-1}$. Studies using Li-doped **22** as an electrode for electrochemical hydrogen storage gave a discharge capacity of 238 $mA\,h\,g^{-1}$, which corresponds to a hydrogen desorption capacity of 0.88 wt %.[129]

4.3. Pentacene Single-Crystal Studies

Early studies of transistor devices fabricated on the surfaces of single crystals of **22** yielded less impressive mobilities than those observed for devices with **1** and **3**. Aside from the issues of material purity, the polymorphism of **22** is also a significant issue in the performance of single-crystal transistors. A recent technique that is able to map changes in crystal-packing phases in single crystals of **22**, lattice-phonon confocal Raman mapping, has allowed the determination of phase inhomogeneities on the micrometer scale and demonstrated that phase boundaries, present to some extent in all crystals studied, extend well into the body of crystals of **22**.[130] Because of the significant difference in band structures for these two phases,[124] the phase boundaries likely represent at a minimum shallow trapping sites for charge carriers. Nevertheless, studies of single-crystal devices with **22** reveal useful information regarding charge injection and transport. One recent study yielded transistors with charge-carrier densities of 10^{11}–$10^{12}\,cm^{-2}$ and showed that hole mobility (ca. 0.5 $cm^2\,V^{-1}\,s^{-1}$) was independent of temperature above 150 K.[131] Another study yielded pentacene-crystal FETs with a hole mobility of 0.3 $cm^2\,V^{-1}\,s^{-1}$,and $I_{on/off}$ values up to 5×10^6. Further analysis of transistor performance led to the conclusion that the number of mobile carriers was only 0.4 % of the number of injected carriers—this information, combined with the observed mobility, implies an intrinsic mobility of tens of $cm^2\,V^{-1}\,s^{-1}$.[132]

Along with issues of polymorphism and crystal quality, one of the issues most commonly cited for the low performance of single crystals of **22** relative to those of **3** and **1** is the purity of the more-reactive pentacene. To this end, the luminescence of single crystals of **22** was studied to determine the nature of impurities leading to trap states in pentacene-based devices.[133] An emission band at 1.49 eV was found to decrease upon purification of the material, and resonance Raman experiments proved that this emission arose from an impurity.

The purification of **22** by sublimation separates several materials: a residue, the pure pentacene, and lighter impurities in the approximate ratio 1:2:1.[134] These lighter impurities include 6,13-dihydropentacene and 6-pentacenone, as well as the known 2:1 cocrystal of dihydropentacene and pentacene[135]. The production of 6-pentacenone and 6,13-pentacenequinone is dramatically increased if the oxygen content of the carrier gas is greater than 2 ppm. MS analysis of the less-volatile residue showed that it contained both peripentacene **31** and trisperipentacene **32**. The formation of **31** requires the loss of five equivalents of H_2; it was postulated that this reaction may be the source of hydrogen

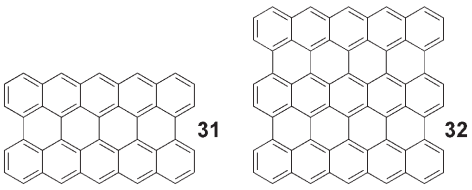

necessary to form the significant quantities of dihydropentacene during the sublimation. The mobility of single-crystal FETs prepared from purified **22** was 2.2 $cm^2V^{-1}s^{-1}$. As the quinone impurity cannot be removed completely, further studies were performed which showed that the quinone impurity lies predominantly at the surface of the single crystals; thus deposition of insulating layers on the crystal surface of **22** led to a nonuniform interface between **22** and the dielectric. This issue was resolved by using a pentacenequinone layer (> 200 nm thick) as the insulating layer. Single-crystal transistors fabricated on **22** with this superior dielectric interface yielded mobilities greater than 15 $cm^2V^{-1}s^{-1}$.[136]

Instead of the reductive decomposition product dihydropentacene, the Palstra group focused on the oxidative decomposition product pentacenequinone as the most significant impurity in **22**.[137] By careful control of the vacuum-sublimation conditions, they were able to remove a significant proportion of pentacenequinone from raw **22** before single crystals were grown by vapor diffusion. The crystals formed from this prepurified **22** were analyzed by HPLC and found to contain 0.028% pentacenequinone. In contrast, high-quality crystals grown from **22** that was not prepurified showed a 0.11% concentration of this impurity. Resistivity measurements on the crystals of **22** showed significant anisotropy across all three crystallographic axes: $\rho_a = 1.3 \times 10^6$, $\rho_b = 4.7 \times 10^5$, and $\rho_c = 2.1 \times 10^8$ Ωm. Analysis of the higher-purity single crystals by the SCLC technique yielded a mobility of 35 $cm^2V^{-1}s^{-1}$ at room temperature and 58 $cm^2V^{-1}s^{-1}$ at 225 K (these values are corrected for effective crystal thickness and for anisotropic resistivity), and the trap-free SCLC transition occurred at a field of approximately 2×10^5 Vm^{-1}. The temperature dependence of the mobility is consistent with bandlike transport.

Significant anisotropy of mobility within the crystallographic *ab* plane of **22** has been observed by both the SCLC technique[138] and by FET measurements,[139] the latter reporting a fourfold difference in mobility across a 90° rotation. Recent calculations of the band structure of **22** by DFT support significant mobility anisotropy in the *ab* plane owing to frustration of hole transport along the crystallographic *b* axis (Figure 17).[140]

Recent single crystal studies have shown that water vapor leads to the formation of discrete trap states when the device is placed under bias.[141] The electronic effects of this trap state only became noticeable after around 100 minutes of bias; this timescale is much longer than that typically utilized for the measurement of FET properties, but is not unusual for devices in real applications. Treatment of the gate dielectric with a hydrophobic monolayer eliminated water at the gate/organic interface, precluding the formation of this trap state. As with the results reported by Lang and co-workers,[133] this

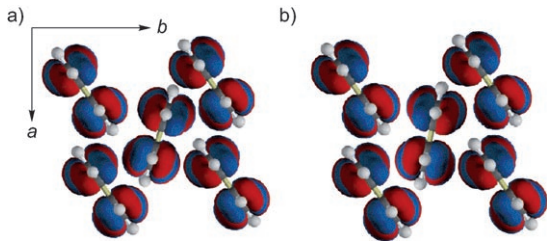

Figure 17. HOMOs of pentacene in the crystal, viewed along the long molecular axis: a) fully bonding situation, as found in the bottom of the valence band. b) partially antibonding interactions found in the top of the valence band, showing frustration along the *b* axis. Figure adapted from reference [140].

behavior seems to indicate diffusion of a small molecule into the crystal lattice to yield the observed trap states; it has been reported recently that water can indeed diffuse into crystals of **22**.[142]

4.4. Pentacene Thin-Film Devices and Their Characterization

Pentacene (**22**) is most commonly used as the semiconductor in thin-film transistors,[143] where it serves as the benchmark against which other organic compounds are measured.[144] The first pentacene transistors, reported by Horowitz et al. in the early 1990s, had a mobility of 0.002 $cm^2V^{-1}s^{-1}$ in a top-contact device.[145] Purification of **22** by sublimation improved the mobility to 0.038 $cm^2V^{-1}s^{-1}$ for a bottom-contact device.[146] With high-purity materials, further optimization of film morphology by employing self-assembled monolayers on the dielectric surface led to dramatic increases in device mobility: greater than 1 $cm^2V^{-1}s^{-1}$ in a bottom-contact device.[147]

Temperature-independent transport in pentacene-based FETs was observed shortly thereafter, although high variability between devices raised issues of traps and electrode contacts as key impediments to high-performance devices.[148] Other approaches to device processing improved as well, with the use of self-assembled monolayers to allow patterning of the pentacene film.[149] Pentacene transistors fabricated with an additional pair of electrode contacts in the device channel allowed the determination of the contact resistance at the **22**/electrode interface.[150] The contact potential drop at the drain electrode was found to be larger than the drop at the source electrode, implying that carrier extraction is not as efficient as carrier injection. Variable-temperature measurements, which give the activation energies for transport, showed that at large gate voltages the contact resistance and channel resistance were essentially identical; thus, differences in contact resistances under normal operating conditions likely arise from differences in the detailed structure of the metal/**22** contacts. Transport activation energies for both contacts and film are in the range 15–40 meV, indicating that contact resistance is strongly related to carrier transport in the film in the area around the electrodes.

Fabricating pentacene-based transistors with the double-gated configurations as shown in Figure 18 allowed the

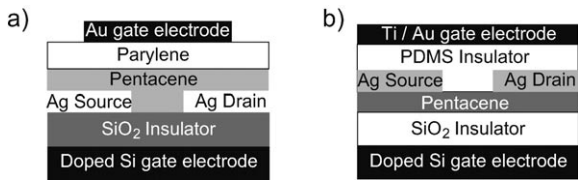

Figure 18. "Stacked" pentacene transistors with parylene (a) and polydimethylsiloxane (PDMS) (b) as insulators.

extraction of transistor properties from a single film of **22** in both top-gate and bottom-gate configurations.[151] The mobilities from bottom-contact measurements ($0.4\ cm^2 V^{-1} s^{-1}$) were slightly higher but of the same order of magnitude as those measured from the top-contact configuration ($0.1\ cm^2 V^{-1} s^{-1}$). The decrease in mobility for the top-contact measurement may arise from the roughness of the top surface of the pentacene film. A similar approach taken by Bao and co-workers used a flexible PDMS stamp based device[152] that conformed readily to the rough top surface of the film. Again, the mobility derived from the bottom of the device was as much as 37% higher than that extracted from the rougher top surface.

As with single crystals of **3**, thin films of **22** were measured for the Hall effect. Using a device configuration similar to that in Figure 10, a Hall voltage as high as 0.7 mV at a field of 9 T was observed. The Hall mobility was calculated to be $0.4 \pm 0.1\ cm^2 V^{-1} s^{-1}$, which is similar to the mobility extracted from analysis of the FET parameters for this device.[153]

4.4.1. *Morphology*

The importance of film morphology has been realized since the earliest reports of high-performance pentacene transistors,[154] and this topic has been the subject of a recent review.[155] Perhaps the most significant issue in this respect is the presence of several polymorphs of **22**. Whereas there are only two reported single-crystal polymorphs, studies of thin films are complicated by the observation of at least four phases of **22**, whose relationship to the single-crystal forms has been investigated in detail.[156] The most distinguishing feature of these polymorphs is their (001) spacing (layer periodicity). X-ray diffraction of thin films can be used to identify the polymorphs on the basis of this repeat distance—the currently known phases yield values of 14.1, 14.4, 15.0, and 15.4 Å. The 14.1-Å polymorph corresponds to most recently determined values for single crystals of **22** and is often referred to as the "bulk" value. Often, more than one polymorph can be observed in evaporated films of **22**, but films of single polymorphs can be prepared by careful control of the substrate temperature and film thickness.[157] A detailed modeling study using the data provided by XRD experiments produced reasonable structures for both the 14.1- and 15.0-Å polymorphs.[158]

The importance of substrate temperature for the growth of highly ordered films of **22** has been known since the 1970s.[159] Detailed real-time studies of the growth of these films on SiO_2 and alkane-monolayer-treated SiO_2 by using synchrotron radiation yielded significant insights into the mechanism of film growth:[160] the growth of the first monolayer of **22** proceeded to completion before the growth of the second monolayer began.[161] Subsequent layers can nucleate before the second monolayer completes its growth, giving rise to the "island" structures observed in pentacene films. Grazing-incidence X-ray diffraction studies of monolayers of **22** showed that the first deposited layer differs significantly in structure from subsequent layers.[162] When the surface was treated with an alkane monolayer, the weaker **22**/substrate interaction allowed molecules of **22** from lower layers to migrate upwards and act as nucleation sites for subsequent layers, leading to 3D growth. More recent studies showed that the precise morphology of the initial monolayer played the key role in determining the transistor performance of films of **22**.[163] The electronic performance of films of **22** also depends on the number of monolayers:[164] hole mobility increased during film growth until six monolayers had been deposited, at which point mobility saturated. The equilibrium structure of these latter layers rapidly approaches that of bulk samples.[165]

When deposited on oxide or organic surfaces, **22** orients with its long axis perpendicular to the substrate. On metal or semiconductor surfaces, in contrast, molecules of **22** align with their long axes parallel to the substrate.[166] Studies of deposition of **22** on crystalline silicon by low-energy electron microscopy demonstrated the growth of large grains of **22** on Si(001) surfaces.[167] FTIR analysis showed that the initially deposited **22** reacts chemically with the Si surface, but this issue could be circumvented by pretreatment of the Si surface with cyclohexene to form an inert organic surface monolayer. Subsequent deposition of **22** yields films with significantly improved uniformity and order.[168]

4.4.2. *Dielectrics*

The dielectric surface has a strong influence on the morphology of the pentacene film deposited upon it, and the nature of the dielectric influences the voltage range over which the device operates. Both organic[169] and inorganic[170] dielectrics can yield transistors with low-voltage operational windows, provided they have smooth surfaces that allow the formation of crystalline films with large grain sizes.[171] Substrate roughness can be ameliorated by coating a surface with a thin film of polystyrene[172] or PMMA.[173] A number of detailed studies have related the dielectric material to the morphology and performance of FETs;[174] a more detailed coverage of the issue of gate insulators and their surface treatment can be found in a recent review.[175] Treatment of oxide dielectrics with self-assembled monolayers can also improve other aspects of device performance, and this approach has also been reviewed recently.[176] Although the most common substrate/monolayer combination is OTS on SiO_2, similar treatments also work well on alumina[177] and zirconia.[178] Variations in the nature of the monolayer on SiO_2 surfaces can alter threshold voltages to as high as 26 V (by treatment with fluorocarbon-based trichlorosilanes, $\mu = 0.15\ cm^2 V^{-1} s^{-1}$) and as low as −12 V (by treatment with phenyltrichlorosilane, $\mu = 0.7\ cm^2 V^{-1} s^{-1}$). AFM and XRD analysis of the films showed no significant morphological

changes, leading the authors to postulate that the monolayer dipole modifies the surface potential of the organic layer adjacent to the dielectric.[179] The threshold voltage has also been decreased by addition of dopant ($FeCl_3$) to **22** beneath the Au electrodes in top-contact devices.[180] The use of a polymer electrolyte dielectric layer allows very-low-voltage operation of pentacene transistors: the current changes by four orders of magnitude over a gate voltage sweep of only 2 V.[181] The benefit of low-voltage operation is countered by the slow response time of the devices as a result of the rate of ion migration in the polymer film.[182]

4.4.3. *Electrode Interfaces*

The interface between **22** and metal electrodes determines the efficiency with which charge carriers are injected and removed from the semiconductor. As a first approximation the metal electrode should have a work function of similar energy to that of the orbital of the organic material into which charge is being injected—the HOMO for holes, the LUMO for electrons. However, numerous other factors complicate the issue. The interaction of closed-shell organic molecules with the polarizable electron cloud on metal surfaces leads to significant changes in the interfacial region,[183] and **22** has been used to probe these interactions. Deposition of **22** on gold was studied by UV photoemission spectroscopy and inverse photoemission spectroscopy, which showed a strong interface dipole with a 0.6-eV shift in the work function of the metal.[184] This shift results in barriers to charge injection of 0.47 eV for holes and 1.17 eV for electrons. Variations in deposition conditions can yield even larger shifts in metal work function,[185] leading to injection barriers of 0.55 eV for holes and 1.3 eV for electrons.[186] The deposition of gold onto a pentacene surface, as is commonly done for top-contact transistors, damages the pentacene film, reducing device reliability and reproducibility[187] and inducing larger interface dipoles (−1.0 eV for gold, −0.7 eV for silver).[188] As in single-crystal studies, gold evaporated onto PDMS stamps can be laminated onto thin films of **22** to avoid damaging the organic layer.[189] It might be expected that organic/organic interactions would eliminate the formation of interface dipoles, but this is not the case with conducting polymer electrodes such as PEDOT/PSS (although the dipole is only −0.25 eV).[190] The authors speculate that this difference arises from fundamental electronic differences between metals and conducting polymers, although other investigations showed that morphological differences between films grown on metals and those grown on organic surfaces may play a crucial role.[191]

Whereas many current synthetic efforts towards organic semiconductors focus on "tuning" HOMO energy levels to match electrode work functions, recent studies show that improving the morphology at the electrode may be equally important.[192] Morphological differences found in the regions around the electrodes, along with a strong dependence of contact resistance on the mobility of the organic films, imply that high contact resistance may arise from limitations on diffusion of carriers in the organic material near the metal surface.[193] The buildup of charge in these regions will lead quickly to space-charge limited injection and high observed contact resistance.

Electrode surface modifications to improve charge injection include exposure of gold to oxygen plasma, which led to a decrease in contact resistance of pentacene films.[194] Morphology studies showed that after oxygen plasma treatment pentacene molecules on a gold surface arranged with their long axes perpendicular to the surface, similar to their arrangement on oxide surfaces. Other studies showed that coverage of gold surfaces with alkane thiols also causes **22** to adopt a vertical orientation in the film.[195] UV photoemission spectroscopy was used to examine hole-injection barriers between **22** and either gold (with chemisorbed chlorine) or PEDOT/PSS.[196] In both cases the pentacene molecules at the surface of the electrode are oxidized to yield surface charge-transfer complexes that improve injection.

A versatile approach to modify gold electrode surfaces is treatment with solutions of electron-deficient arene thiols to cover the electrode with an aromatic layer.[197] Treatment of Pd electrodes with 4-nitrobenzenethiol led to improved transistor performance,[198] and treatment of gold electrodes with arenes such as 2-mercapto-5-nitrobenzimidazole decreased contact resistance to as little as 50 kΩ.[199]

4.4.4. *Traps and Defects*

The mobility in organic FETs is limited by carrier traps in the semiconductor film. Deep trap sites typically arise during device fabrication, whereby deposition of gate dielectric or electrodes can cause significant damage,[200] whereas other defects arise upon exposure of the pentacene film to air and light. The most commonly cited trapping states in polycrystalline films are the boundaries between pentacene grains, although studies by synchrotron X-ray diffraction,[201] along with studies of FET performance under a variety of conditions, point to intragrain defects as the most significant trapping sites.[202] The positive turn-on voltage in these devices was cited as evidence for trap states that are electron accepting (e.g. pentacenequinone). Electric force microscopy was used to observe and image long-lived (ca. 30 s) trapped charges in pentacene thin-film transistors[203] and showed that defect sites are distributed inhomogeneously in the film, but are not particularly localized at grain boundaries. Grain size is certainly not irrelevant. Very small grains with numerous boundaries are detrimental to device performance,[204] but mobility does not correlate linearly with number of grain boundaries—rather, for average grain sizes below 2 μm, mobility drops abruptly.[205] Investigation of pentacene films performed by lateral force microscopy combined with Kelvin probe force microscopy[206] showed that grain boundaries do serve as charge-carrier traps, but with depths on the order of only 5–10 meV.

Trapping sites can also arise during operation of organic devices, as large current densities flow through very thin layers of the pentacene film. Studies during SCLC measurements on crystals of **22** showed the appearance of a defect in the material with a trap energy of 380 meV.[207] Allowing the sample to stand for several hours at room temperature (or irradiation at 420 nm) caused this defect to disappear. The

kinetics of this process were consistent with atomic diffusion, perhaps arising from protonation of **22**. A further study of pentacene films evaporated on glass showed that after prolonged bias, sodium ions began to diffuse into the pentacene layer, thus doping it.[208]

Another trapping phenomenon arises from subtle defects in the crystalline order of **22**. Small shifts along its the long axis only minimally perturb the overall packing (Figure 19), but have been calculated to create relatively shallow (ca. 100 meV) traps in the electronic structure.[209] STM analysis of highly ordered pentacene films showed that the pentacene molecules stick up by as much as 1.2 Å above the plane. The "mole hills" arising from these defects can occupy as much as 20% of the monolayer surface.

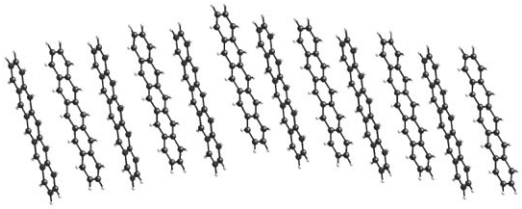

Figure 19. Slip-dislocations in pentacene films. Adapted from reference [209].

4.4.5. *Stability*

Pentacene transistors commonly suffer from bias stress effects, whereby the threshold voltage shifts over time. This effect appears to depend on the thickness of the pentacene layer, indicating that buildup of charge trap sites in the non-active region of the pentacene film is a possible cause.[210] Several recent studies have explored other factors that influence the long-term performance of pentacene-based devices.[211] Pentacene transistors with short channel lengths and high current densities show the most significant decrease in performance after prolonged operation. Devices measured under oxygen-free nitrogen show much less degradation, as do devices formed on dielectrics that allow lower voltage operation, even though they also function at high current densities. These results hint at a thermally induced reaction between **22** and oxygen.[212] No significant changes were observed in films of **22** upon exposure to oxygen at room temperature (although exposure to small amounts of ozone did lead to oxidation of **22**).[213] Exposure of pentacene FETs to oxygen in the dark elicited only a small change in the threshold voltage V_{th} for hole injection, whereas exposure to oxygen and light caused significant changes to V_{th} and the drain current.[214] FETs fabricated on silica showed decreased drain current and mobility with increasing humidity as a result of accumulation of water molecules at the dielectric interface.[215] Similarly, devices formed on highly polar poly(vinyl phenol) (PVP) showed a reversible increase of drain currents on exposure to humidity, likely because of adsorbed water molecules at the interface.[216]

4.4.6. *Pentacene as an n-Type Semiconductor*

To fabricate a wider array of semiconductor devices, several approaches have been taken to induce n-type behavior in pentacene (**22**). Theoretically, efficient electron as well as hole conduction in **22** is supported by the similar magnitude of calculated HOMO and LUMO band widths.[217] Studies of pentacene films by conducting-probe AFM showed that both electrons and holes could be injected into pentacene monolayer islands, and that both carrier types delocalized throughout the island.[218] Early approaches to ambipolar transistors have used **22** as the p-type material in bilayer devices—these are typically fabricated using either a fullerene[219] or perylene diimide[220] as the n-type material. However, in these cases **22** is exploited for its high hole, rather than eletron, mobility.

The n-type behavior of **22** could be realized by deposition of a 0.6-nm-thick film of Ca on top of the dielectric, which fills electron traps present at the dielectric/semiconductor interface. This Ca buffer layer is then covered with the **22** as a semiconductor, and Ca electrodes are used in a top-contact configuration (Figure 20a). The electron mobility under inert

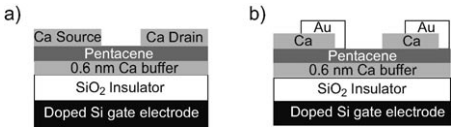

Figure 20. Pentacene as an n-type semiconductor with Ca electrodes and buffer layer.

atmosphere was measured to be 0.19 $cm^2 V^{-1} s^{-1}$.[221] A similar approach was used to yield ambipolar pentacene transistors (Figure 20b), the electrode pattern of which allows a choice of metal contacts for use as the source or drain electrodes. In this arrangement, hole and electron mobilities on the order of 0.1 $cm^2 V^{-1} s^{-1}$ were obtained.[222] A similar principle was used in the fabrication of a pentacene-based inverter circuit.[223]

Although it has been recently reported that gate dielectrics containing hydroxy groups preclude the observation of n-type behavior in organic polymer semiconductors,[224] recent reports describe ambipolar behavior in pentacene layers grown on poly(vinlyl alcohol) (PVA) gate dielectrics; gold was used for the source and drain electrodes.[225] The key parameter was the use of a gate dielectric that yielded appropriate film morphology at the electrode surfaces. With optimum morphology, even the large electronic barrier between the gold electrode and the LUMO energy of **22** (ca. 1.35 eV) could be overcome to yield devices with hole mobility of 0.5 $cm^2 V^{-1} s^{-1}$ and electron mobility of 0.05 $cm^2 V^{-1} s^{-1}$. Ambipolar pentacene devices on PVA have been used to create inverter circuits with **22** as the only semiconductor.[226]

4.4.7. *Applications and Unusual Device Configurations*

Although this review focuses on the intrinsic properties of pentacene (**22**), it is impossible to overlook the remarkable

contributions **22** has made to the development of organic-based electronics. The mild conditions required to deposit films of **22** has allowed the exploration of unusual substrates for the fabrication of semiconductor devices, such as paper[227] or other flexible substrates,[228] and pentacene transistors have been patterned onto weavable fibers[229] and optical fibers,[230] and have been fabricated by using electrodes on flexible stamps,[231] by microcontact printing,[232] and transfer patterning.[233] Excellent performance has been attained on a variety of substrates by using conducting polymer[234] or single-walled carbon nanotube[235] electrodes. Electron-beam lithography has allowed the preparation of transistors in sizes from 10 to 30 nm.[236]

A unique approach to improving transistor mobility involved the deposition of single-walled nanotubes in the device channel. The concentration of nanotubes is controlled to form a nonpercolating network to avoid creating short circuits between the source and drain electrodes.[237] Pentacene is subsequently deposited on top of the nanotube array (Figure 21). The mobilities obtained with this procedure were

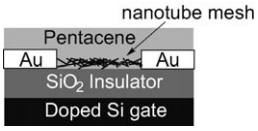

Figure 21. Single-walled nanotube/pentacene transistor.

two times higher than those obtained when nanotubes were not in the channel.[238] Alternatively, chemical doping can be used to increase the number of carriers available in the device channel. Evaporating a thin film of the organic acceptor tetrafluorotetracyanoquinodimethane over the pentacene layer in the channel leads to charge-transfer interactions that add carriers to the semiconductor film.[239] By carefully controlling the proportion of the channel covered by the acceptor molecule, the authors were able to vary the threshold voltage selectively over a range of 50 V.

Pentacene films have been generated by neutral cluster beam,[240] supersonic beam,[241] and pulsed UV laser deposition.[242] A variety of molecular beam deposition methods have also been employed, allowing control over the kinetic energy of the pentacene molecules as they impact the substrate.[243] Recent research has been directed at methods to reduce "overspray" of vapor-deposited pentacene to economize the use of this expensive material and to yield patterned films. Careful control of deposition pressure, substrate temperature, and dielectric treatments allowed the selective growth of pentacene on device substrates to yield well-defined transistors with mobility up to 1.2 $cm^2 V^{-1} s^{-1}$.[244] Analogous to ink-jet printing, hot vapor jet printing uses a carrier gas and a nozzle to deposit the pentacene onto the substrate, and a variety of parameters can be varied to improve pattern resolution and film quality[245] to yield resolution up to 1000 dpi and mobilities as high as 0.25 $cm^2 V^{-1} s^{-1}$.

Pentacene has been used in bistable[246] and nonvolatile memory devices[247] and is amenable to a variety of diode and other device structures for use in RFID tags,[248] inverters,[249] ring oscillators,[250] and other logic circuits.[251] The sensitivity of films of **22** to a variety of analytes have led to their use as sensors.[252] Changes in pentacene device mobility as a function of applied external pressure[253] has been used to create mechanical force and pressure sensors,[254] as well as conformable pressure sensors.[255] Pentacene monolayers were found to improve wetting and crystallinity of subsequently deposited C_{60} layers, leading to improved performance of fullerene transistors (electron mobility up to 2 $cm^2 V^{-1} s^{-1}$).[256] One of the most anticipated applications for pentacene transistors is in active-matrix displays. A number of prototype devices have been reported, including liquid crystal,[257] OLED,[258] and electrophoretic displays.[259]

4.4.8. Pentacene Solar Cells

Photophysical studies[260] show that **22** is suitable for use in solar cells.[261] Single-heterojunction solar cells have been fabricated with a **22**/C_{60} interface.[262] The configuration of the device is similar to that for tetracene solar cells (Figure 12), consisting of a 45-nm pentacene layer, a 50-nm C_{60} layer, and a 10-nm bathocuproine layer. Under illumination (100 $mW cm^{-2}$), the device produced an impressive short-circuit current of 15 $mA cm^{-2}$, an open-circuit voltage of 0.363 V, and a fill factor of 0.5. These values led to an overall power conversion efficiency of 2.7%. Thermal annealing of **22**/C_{60} solar cells leads to improved efficiency as a result of small increases in built-in potential and significant increases in photocurrent—the latter is likely due to improvement of molecular ordering of both pentacene and C_{60} upon annealing.[263] The high reactivity between **22** and fullerenes leaves some concern about the possibility of reaction between donor and acceptor at the important interface between the two materials, and this may impact device lifetime. A few researchers are already exploring other acceptor species for use with **22**. As with formation of ambipolar transistors, co-evaporation of **22** and perylenediimide compounds leads to an interpenetrating network that can also be used for solar energy conversion. In this case, measurement under AM 1.5 conditions in an inert environment showed a power conversion efficiency of 0.54%.[264]

4.5. Functionalized Pentacene

4.5.1. Reversible Functionalization

One way to replicate the electronic properties of **22** in a solution-cast film is to prepare the film from a soluble precursor that can be converted into **22** after the film has formed. The ideal approach requires a soluble precursor with good film-forming properties, a conversion reaction that takes place under mild conditions, and an addend sufficiently volatile to be completely and easily removed from the forming pentacene film.

Müllen and co-workers first reported a device fabricated from precursor-route **22** in 1996 (Scheme 4).[265] Solutions of compound **33** formed high-quality films by spin-casting onto the surface of a bottom-contact FET device. Heating the

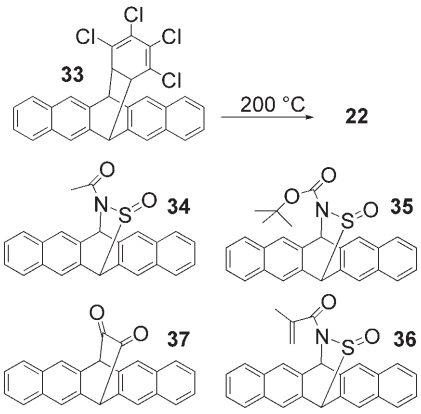

Scheme 4. Reversibly functionalized pentacene derivatives.

precursor film at 200 °C for 5 seconds yielded the acene film, which formed transistors with mobilities as high as 0.2 $cm^2V^{-1}s^{-1}$ and on/off current ratios of 10^6. An alternative series of approaches use *N*-sulfinylamide groups (**34**–**36**), which have a numbed of advantages: ease of synthesis of the functionalized pentacene, ease of removal of the group, and the ability to tune the properties of the material by altering the group attached to the amide. Derivative **34** yielded devices with hole mobility as high as 0.9 $cm^2V^{-1}s^{-1}$ after annealing at 200 °C,[266] and derivative **36** formed films that could be easily photopatterned.[267] Using a slightly different, acid-labile solubilizing group (**35**) allowed photopatterning of films with the assistance of a photoacid-generating dopant to create patterned transistors with mobility as high as 0.2 $cm^2V^{-1}s^{-1}$.[268] These soluble precursor-route pentacenes have been used to demonstrate device fabrication by ink-jet printing,[269] as well as the fabrication of display backpanes.[259] An alternative approach to photopatternable films of pentacene involves the use of solubilizing groups that can be removed by irradiation, as exemplified by diketone **37**.[270] This soluble compound is converted back into pentacene by irradiation at 460 nm (the authors also report the high-yield formation of dibromopentacene films by this method). Although the conversion into pentacene needs to take place under an inert environment to prevent formation of the endoperoxide, the method provides an efficient, low-temperature method to generate pentacene thin films, and offers the potential of patterning the film by appropriate focus of the light beam used to generate the pentacene.[271]

4.5.2. Aryl Pentacenes

6,13-Diphenylpentacene (**38**) and 5,7,12,14-tetraphenyl pentacene (**44**), first prepared in the 1940s,[272] are the earliest reported functionalized pentacenes. 6,13-Diaryl pentacenes are in general both more stable and more soluble than the parent compound beacuse of substitution on the most reactive position of the acene.

However, diaryl pentacenes remain potent dienes—**38** reacts rapidly with C_{60} to form a covalent adduct. A significant number of diaryl pentacenes have been prepared,[273] and a number have found application as red-emitting dopants for OLEDs;[274] their saturated red emission lead to devices with external quantum efficiencies as high as 1.4% (for **43**, Figure 22).[274b] A few studies of transistor applications of diaryl pentacenes have been performed. In general, the additional edge-to-face interactions possible in diaryl pentacenes such as **38** (Figure 22) lead to minimal π overlap and thus poor transistor performance.[275] Dithienylpentacene (**40**), in contrast, adopts a π-stacking arrangement in the crystal to yield thin-film transistors with mobilities of 0.1 $cm^2V^{-1}s^{-1}$.[276]

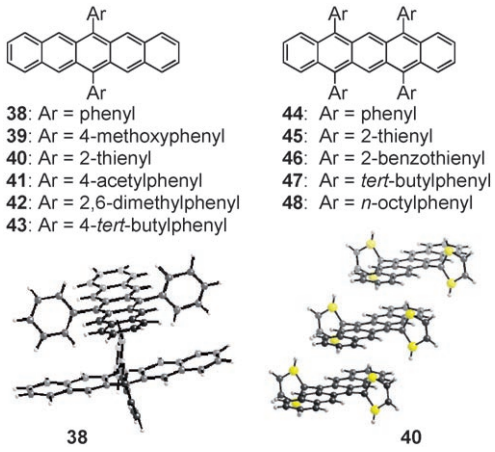

Figure 22. Aryl-functionalized pentacenes, and the crystal packing of **38** and **40**. See the supplementary information for reference [276].

4.5.3. Alkyl Pentacenes

Relatively few alkyl-substituted pentacenes have been reported, as this substitution tends to lower the oxidation potential of this aromatic system, which further decreases environmental stability. One of the few examples in this class is 2,3,9,10-tetramethylpentacene (**49**),[277] which crystallizes in a typical acene herringbone arrangement and yields vapor-deposited transistors with hole mobility as high as 0.3 $cm^2V^{-1}s^{-1}$ (on/off current ratio of 6×10^3).

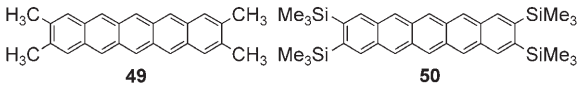

The similar 2,3,9,10-tetrakis(trimethylsilyl)pentacene (**50**) highlights a significant issue with pentacene derivatives lacking substituents on the central aromatic ring. This compound is highly soluble and has an oxidation potential of 725 mV (vs. SCE), but is poorly stable, surviving only a week in deoxygenated solution. The low stability precluded device fabrication or acquisition of the crystal structure of the pentacene itself, but the main decomposition product (the butterfly dimer) could be analyzed crystallographically.[278]

Alkyl-substituted pentacene **52** was the product of a metal-mediated iterative synthesis (Scheme 5). Beginning with phthalate ester **51**, repeated application of a zirconium-

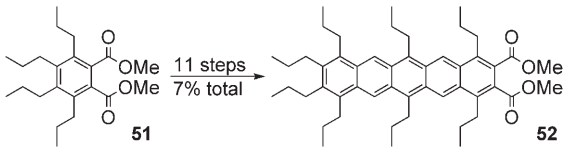

Scheme 5. Reiterative synthesis of pentacene **52**.

mediated cyclization in an 11-step process yielded the product. Little discussion of the properties of this pentacene derivative was presented, but it was soluble and stable enough to be characterized by ^{1}H and ^{13}C NMR spectroscopy.[279]

4.5.4. *Halogen-Substituted Pentacene*

Tetrachloropentacene **53** was prepared as part of the search of new materials for organic FETs.[280] Although **53** was insoluble and difficult to characterize, satisfactory confirmation of structure was obtained by mass-spectrometric and combustion analyses. Compound **53** did not yield functioning FET devices owing to polymerization of the compound upon attempted thermal evaporation (Scheme 6). Examination of the thermochemistry of **53** showed sequential loss of pairs of chlorine atoms to give benzyne-like species, which reacted with adjacent pentacene molecules to form an ypticene-based carbon network. When **53** was heated to above 900 °C, it formed a carbonaceous solid with a conductivity greater than 5 $S\,cm^{-1}$.

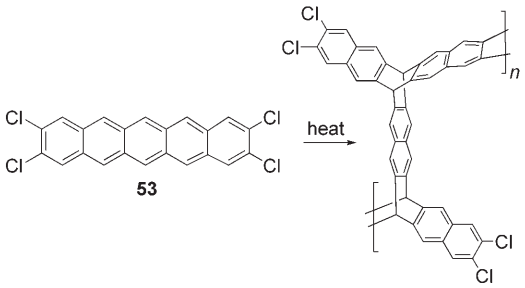

Scheme 6. Polyypticene formed by the thermal decomposition of 2,3,9,10-tetrachloropentacene (**53**).

Another halogenation strategy led to perfluoropentacene **54**, which crystallized in a herringbone motif similar to that adopted by pentacene, although with a nearly 90° edge-to-face angle (compared with 52° for pentacene; Figure 23).[281] Perfluorination also shifted the reduction potential by almost 800 mV to approach the value measured for C_{60}.[282] Transistor

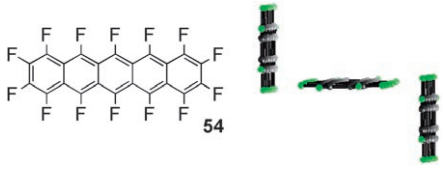

Figure 23. Perfluoropentacene (**54**) and its edge-to-face interactions (CSD code: BEZLUO).

devices fabricated from **54** exhibited n-type behavior and electron mobilities as high as 0.22 $cm^2\,V^{-1}\,s^{-1}$. The synthesis of perfluorotetracene has also been reported.[283]

4.5.5. *Thiopentacenes and Pentacene Ethers*

The oxidation potential of pentacene can be lowered significantly by substitution with π-electron-donating groups such as oxygen or sulfur. 1,4,8,11-Tetramethoxypentacene (**55**) is moderately stable (solutions of this material bleach within one hour) and exhibits two reversible oxidation waves in cyclic voltrammetry (at 0.13 V and 0.54 V vs. ferrocene/ferrocenium).[284]

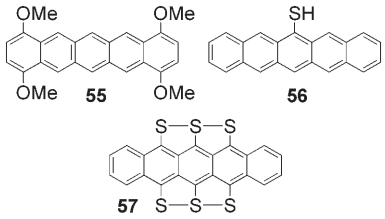

By exploiting the well-known affinity between thiols and gold, 6-pentacenethiol (**56**) was used as a gold electrode surface treatment in nanoscale thin-film transistors. Pentacene was then deposited over this layer by a precursor route, and the films were converted into pentacene by heating (200 °C, 2 min). The field-effect mobility measured from films formed with pentacenethiol-treated electrodes was two orders of magnitude higher than that of devices with no electrode pretreatment.[285] Pentacene derivatives with alkanethiol groups at the 6,13-positions have also been prepared, but device studies on these molecules have not been reported.[286] In contrast, hexathiapentacene **57**, prepared by reaction between **22** and sulfur,[287] has been the subject of recent device studies. X-ray crystallographic analysis of **57** showed that it adopts strongly π-stacked arrays with close sulfur–sulfur contacts between the stacks. Top-contact FETs fabricated from evaporated thin films of **57** yielded mobilities as high as 0.04 $cm^2\,V^{-1}\,s^{-1}$ and on/off current ratio as high as 10^7.[288]

4.5.6. *Ethynyl Pentacenes*

Alkyne-functionalized pentacenes comprise one of the most synthetically accessible classes of functionalized pentacene. Addition of ethynyllithium (or ethynyl Grignard reagent) to pentacenequinone and treatment of the resulting diol with tin(II) chloride yields the desired pentacene in good yield (Scheme 7).

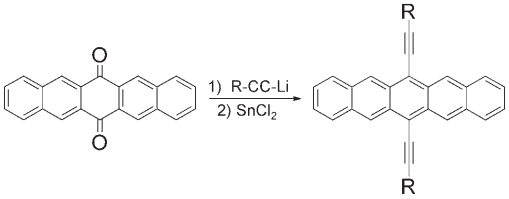

Scheme 7. General synthesis of ethynyl pentacenes.

Phenylethynyl-substituted pentacenes (**58**, **59**) are among the earliest reported functionalized pentacenes. These materials were prepared because of their bright red fluorescence for chemiluminescent systems.[289] The high reactivity of these

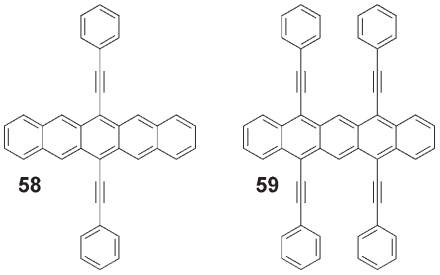

systems has been favorably exploited in their reactions with fullerenes, which has allowed the study of π–π interactions of fullerene adducts.[290] More recently, phenylethyne-substituted pentacenes have been scrutinized for use in FETs. Hexamethoxy derivative **63** (Figure 24), for example, was

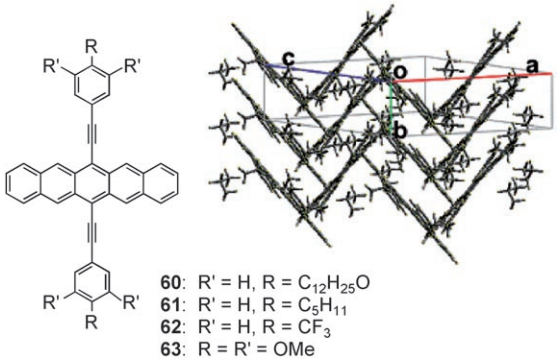

Figure 24. Phenylethynyl pentacenes for FET studies, and crystal packing of **61**. (Adapted with permission from reference [292]. Copyright 2006 American Chemical Society.)

prepared as a soluble pentacene derivative with electron-rich pendants that might also participate in the charge-transport process.[291] Although the crystal structure of this derivative was not reported, the large bathochromic shift in absorption for thin films of this compound (> 30 nm with respect to solution absorption) denotes strong electronic interactions in the solid state. Spin-cast films of **63** led to stable FETs with mobility as high as $2\times10^{-5}\,cm^2V^{-1}s^{-1}$. Derivatives **60**–**62** were also prepared in a search for soluble pentacene derivatives for FETs. Neither compound **60** nor **62** yielded uniform films from solution, but compound **61**, which was found to adopt strongly π-stacked arrangements by single-crystal X-ray analysis (Figure 24, right) did yield highly crystalline films. Top-contact devices fabricated on these films yielded mobility as high as $0.52\,cm^2V^{-1}s^{-1}$.[292]

The use of roughly spherical trialkylsilyl groups as the substituents on the alkyne allows exquisite control over the solid-state arrangement of the pentacene molecules, along with dramatic increases in stability and solubility[293] (although solutions and amorphous films of the materials are still susceptible to "butterfly" dimerization).[294] The strong π-stacking interactions are controlled by the size of the substituent: for small groups (e.g. trimethylsilyl, triethylsilyl derivatives (**64**)), in which the diameter of the substituent is significantly smaller than half the width of the acene, one-dimensional π stacks are formed (Figure 25, upper right).

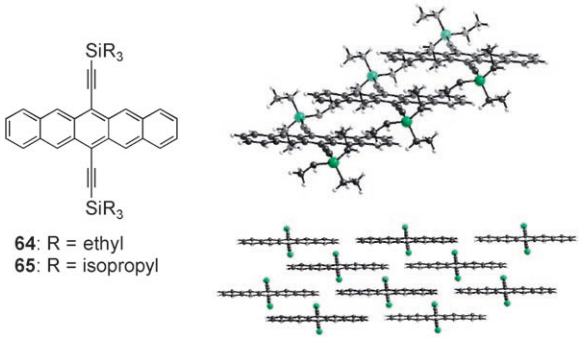

Figure 25. Silylethyne-functionalized pentacenes with typical "small-substituent" (top right) and "large-substituent" (bottom right, shown without alkyl groups on Si for clarity) crystal packing.

When the size of the substituent matches roughly half the width of the acene (e.g. in **65**), a two-dimensional brickwork arrangement is favored (Figure 25, bottom right).[295] The two-dimensional stacking arrangement was found to be optimal for use in FETs: for derivative **65**, hole mobilities as high as $0.4\,cm^2V^{-1}s^{-1}$ were reported for films formed by vacuum deposition,[296] whereas solution deposition (whereby the material is able to form highly crystalline flims) yielded devices with hole mobility as high as $1.5\,cm^2V^{-1}s^{-1}$ ($I_{on/off}=10^7$ and $V_{th}\approx3$ V),[297] a value similar to that found in single crystals of **65** grown across source-drain electrodes of a prefabricated transistor.[298] Pentacene **65** has also been used in a pentacene/C_{60} photovoltaic device to yield a white-light power conversion efficiency of 0.52 %.[299] A number of studies have elucidated a variety of properties for **65**, including a low-temperature phase transition,[300] and all-optical measurements of the carrier mobility show that this compound should have transport properties similar to unsubstituted pentacene,[301] provided appropriate film morphology is attained.[302] These measurements are supported by band-structure calculations, which show significant dispersion in both valence and conduction bands.[303] A more recent study showed that thermal motions in the crystal led to perturbations in intermolecular geometry sufficient to yield significant changes in electronic coupling between molecules, complicating attempts to correlate crystal packing with transport properties.[304] Evidence for long-lived trapped states in photoexcited **64** has been reported,[305] along with persistent photoconductivity that may arise from trapped charge carriers.[306]

The diene reactivity of **65** led to its use as a soluble precursor for the formation of ypticene-based polymers (**68**), highly attractive candidates for organic sensors in which the functionality can be tailored to detect small molecule organic

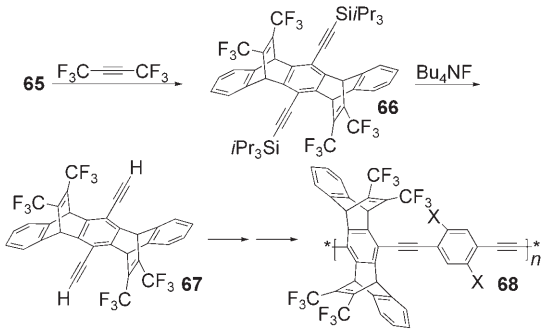

Scheme 8. Pentacene-based polymer synthesis for sensors. X = alkyl, alkoxy, aryl, etc.

compounds[307] or molecules of biological interest[308] (Scheme 8).[309]

4.5.7. *Functionalized Ethynylpentacenes*

Substitution of 6,13-diethynylpentacenes with additional alkyl[310] or ethynyl[311] groups at the 2,3,9,10-positions has been demonstrated as a method to alter the redox properties and HOMO–LUMO gaps of these materials—although FET devices have not been reported for these compounds. A series of stable pentacene ethers have also been reported (Figure 26),[312] exhibiting even lower oxidation potentials

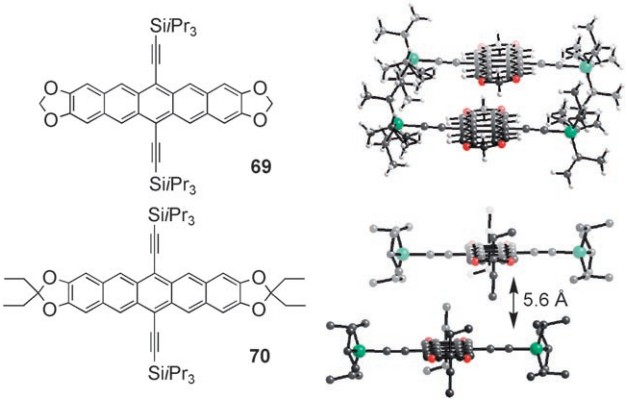

Figure 26. Pentacene ethers **69** and **70**, and their crystal packing.

(as low as 560 mV vs. SCE). Dioxolane-functionalized pentacene **69** also exhibited interesting optical phenomena—the absorption and emission were significantly blue-shifted relative to that of **65**, leading to fluorescence in a region useful for formation of red OLEDs (626 nm). Further, dioxolane substitution led to a significant increase in the fluorescence quantum yield (60 %).[313] Exploitation of **69** as a red-emissive dopant for Alq_3-based OLEDs was hindered by the strong π-stacking interactions, which broadened the solid-state emission. The addition of alkyl (in this case, ethyl) groups to the dioxolane ring increased the separation between pentacene planes in the solid state, and this material (**70**) yielded Alq_3 host/**70** guest OLED devices with bright red emission and an external electroluminescence quantum yield of 3.3 %. This value is very close to the theoretical maximum[314] and also very close to the best values reported (3.6 %)[315] for a small-molecule organic red-emissive OLED.

4.5.8. *Electron-Deficient Ethynylpentacenes*

In the pursuit of soluble n-type pentacenes for complementary logic circuits, ethynylpentacene **71** was further functionalized with electron-withdrawing groups. Nitrile-

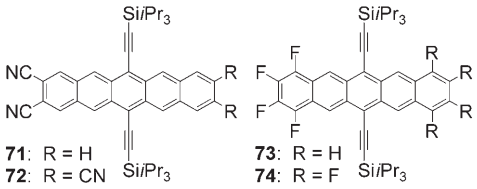

substituted pentacenes **71** and **72** showed significantly decreased reduction potentials (as low as −0.49 V vs. SCE), but poor solubility precluded formation of uniform films for transistor studies. The fluorinated derivatives **73** and **74** showed similarly low solubility, but were amenable to film formation by vacuum depositon. Because the devices were measured in air, no n-type behavior was observed, but hole mobility was found to scale with the number of fluorine atoms on the aromatic ring.[316] This increase in mobility arises from the closer spacing of the fluorinated pentacene uints in the crystal relative to the nonfluorinated derivative.

5. Higher Acenes

Whereas larger acenes such as hexacene and heptacene are not found in petroleum deposits (as are naphthalene and anthracene), or in diesel exhaust and charred food (like tetracene and pentacene), there is evidence of these materials in volcanic ash[317] and in interstellar dust.[318] Acenes larger than pentacene hold considerable promise for use in electronic devices; studies at various levels of theory have predicted that band-gap and reorganization energies will decrease with increasing acene length, whereas the density of states will increase, promising improved carrier mobility.[7] The inaccessibility of acenes larger than hexacene has elicited a host of theoretical investigations of their potential properties, as well as the likely electronic characteristics of polymeric acenes. It has been predicted that acenes as small as heptacene may possess a singlet diradical ground state,[319] whereas predictions regarding the HOMO–LUMO gap of the corresponding polymer (polyacene) span the range from a potential superconductor[320] to a relatively large-gap (0.4 eV) semiconductor.[321] The theoretical studies on the nature of aromaticity and potential electronic properties of larger acenes (and the corresponding polymer) have been expertly covered in a recent review article.[33]

5.1. Hexacene

The synthesis, characterization, and device applications of acenes larger than pentacene are all stymied by their low

solubility, poor light and oxygen stability, and extremely difficult synthetic approaches. Hexacene was first prepared by lengthy Diels–Alder approaches requiring the loss of as many as nine equivalents of H_2 in the final step.[322] A more recent synthesis (Scheme 9) began with reduced quinizarin **75**, which was condensed with naphthalene-2,3-dicarboxaldehyde to yield dihydroxyhexacenequinone **77** in good yield. Reduction with Zn/H_2 yielded dihydrohexacene **78**, and dehydrogenation at high temperature over CuO under vacuum provided hexacene (**79**).[323]

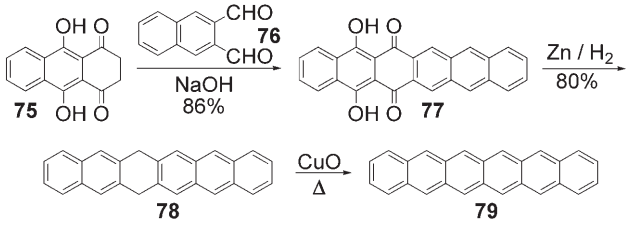

Scheme 9. Synthesis of hexacene (**79**).

The single-crystal X-ray diffraction data for hexacene were weak and the only conclusion that could be made regarding the structure was that it adopted a molecular ordering analogous to that adopted by pentacene and tetracene.[324] Hexacene was sufficiently soluble for the acquisition of absorption spectra (both ground state and triplet state), as well as the spectra of its radical cation, radical anion, dication, and dianion.[325] Accurate studies were hampered by the extremely low solubility of this material, making the determination of extinction coefficients impossible. However, by using degassed silicone oil as solvent, with the temperature held at 300 °C, the absorption spectrum between 200 and 700 nm could be determined. Flash-photolysis studies provided the transient absorption for the triplet at 550 nm. From the absorption spectra, the authors were able to estimate a triplet energy for hexacene of approximately 50 kJ mol^{-1}. Extrapolation by plotting triplet energy versus singlet excitation energy for the acene series from benzene to hexacene led to the conclusion that nonacene could possess a triplet ground state.

One-hundred-nm-thick films of hexacene grown by vacuum sublimation have been doped with both alkali metals and halogens. Doping of these films with I_2 led to an increase in conductivity up to 0.03 S cm^{-1},[326] whereas potassium- and rubidium-doped hexacene exhibited conductivities of only roughly 10^{-5} S cm^{-1}. Thermoelectric power measurements confirm the n-type nature of the Rb-doped material.[327]

5.2. Heptacene

Acenes larger than hexacene have proven elusive. Although Clar[328] and Marshalk[329] reported approaches to heptacene in the 1940s, as did Bailey and Liao in the 1950s,[330] the characterization of these materials was not adequate to confirm the proposed structure completely, and none of these syntheses have been reproduced. The lack of success in the synthesis of heptacene over the last 60 years has led to the conclusion that these larger parent acenes will not likely be isolated in a pure state.[331]

The lengthy drought in approaches to the synthesis of heptacene was recently broken with the isolation of photogenerated heptacene (**81**) in a polymer matrix. Employing the same precursor technique as that used to solubilize pentacene for transistor applications,[270] Neckers and co-workers were able to form **81** by irradiation ($\lambda = 395$ nm) of a 3 mM dispersion of **80** in a PMMA matrix (Figure 27).[332] The lifetime of **81** in the matrix was less than four hours,

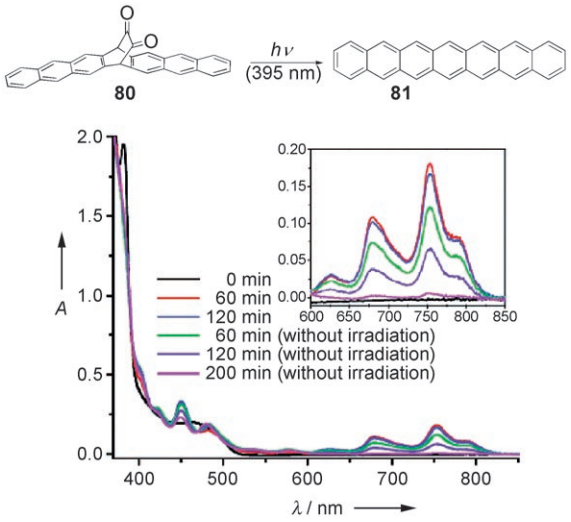

Figure 27. Photogeneration of heptacene in a polymer matrix (top) yields films from which the absorption spectrum of this elusive hydrocarbon can be acquired (bottom). (Adapted with permission from reference [333a]. Copyright 2006 American Chemical Society).

confirming the high reactivity of this compound, and the material could not be isolated if the irradiation of **80** was performed in toluene rather than in the solid matrix. However, absorption spectroscopy of the thin film of photogenerated **81** in PMMA yielded a long-wavelength absorption band at 760 nm, which is considerably different from the band at 836 nm reported by Clar for material prepared in 1942,[328] but corresponds better to the value extraploated from the series from naphthalene to hexacene.

5.3. Functionalized Higher Acenes

5.3.1. Hydroheptacenes

The low solubility and stability of **79** and **81** requires the use of functional groups to stabilize and solubilize these materials if they are to be used in electronic devices. The first challenge is the development of appropriate synthetic approaches for functionalized hexacenes and heptacenes. By analogy with the successful dehydrogenation approaches to hexacene, a few modern syntheses of hydroheptacene have been reported, although none of these approaches led to

isolated heptacene derivatives. Reduction of heptacenequinone **82** (Scheme 10) yielded dihydroheptacene **83** containing two electronically isolated anthracene units. Such materials are efficient blue emitters that may find use in OLEDs. Similar dihydro- and tetrahydroheptacenes have also been used in the preparation of ypticene-based materials.[333]

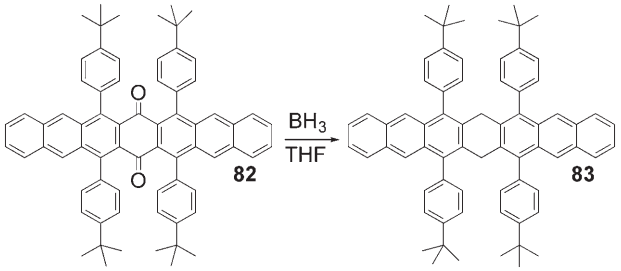

Scheme 10. Reduction of tetra(*tert*-butylphenyl)heptacenequinone to yield the strong blue-emissive dihydroheptacene derivative **83**.

The rapid reaction between fullerenes and acenes has been used to "trap" phenyl-substituted heptacene by forming this reactive species in the presence of C_{60} (Scheme 11).[334]

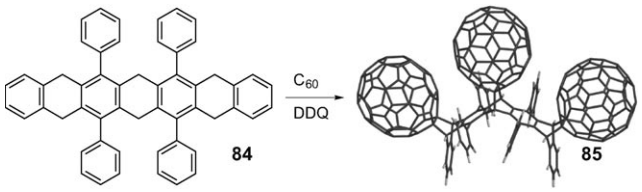

Scheme 11. Synthesis of tetraphenylheptacene–tris(fullerene) adduct **85**. DDQ = dichlorodicyanoquinone.

Treatment of hexahydroheptacene derivative **84** with DDQ in the presence of excess C_{60} led to the isolation of adduct **85** in 20% yield. Although it is possible that heptacene formed in solution before reaction with the fullerene, it is more likely that dehydrogenation and reaction with fullerene proceeded in a stepwise fashion.

5.3.2. *Acenequinones*

Analogous to the syntheses of **22** and **1**, acenequinones are attractive precursors to larger acenes. Although a wide variety of such systems have been reported (many having useful properties such as precursors to polymeric materials or near infrared dyes[335]), their conversion into heptacene (**81**) or larger acenes has not been successful. Alkyne adducts of heptacenequinone (**86**) have been used to form polymers (**87**) by photoinduced "butterfly" dimerization (Scheme 12).[336]

5.3.3. *Silylethyne-Substituted Heptacenes*

The observation that silylethyne-substituted pentacenes were significantly more stable than the unsubstituted hydrocarbon led to the application of this strategy to the preparation of larger acenes. Addition of lithium triisopropylsilylacetylide directly to both 6,15-hexacenequinone and 7,16-heptacenequinone provided the expected diols **88** and **89** in good yield (Scheme 13). A variety of methods were employed to convert these materials into the desired acenes, but none were successful.[337]

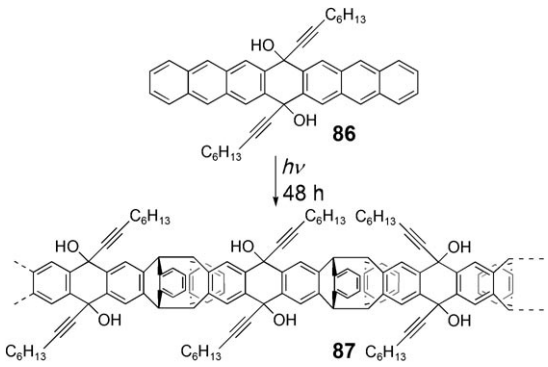

Scheme 12. Synthesis of ladder-type polymer **87** from monomer **86**, accessible by alkynyllithium addition to heptacenequinone.

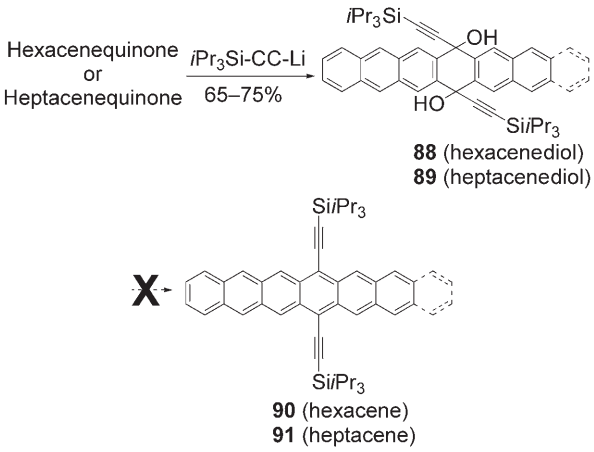

Scheme 13. Acenequinone approach to higher acenes.

To ascertain whether the desired heptacene was being formed under the reaction conditions, the deoxygenation of **89** using tin(II) chloride was attempted in the presence of a large excess of tetracyanoethylene (TCNE; Scheme 14). The major product of this reaction was TCNE adduct **92**.[338] The location of the added dienophile (the heptacene C ring) provides clear evidence for the formation of heptacene. Had the TCNE reacted with the anthracene chromophores of the starting material, it would have preferentially reacted with the central ring of the anthracene unit[339] leading to a heptacene adduct substituted on the B ring.

The high diene reactivity of the larger acenes contributes to much of the instability seen in these systems. Although the triisopropylsilyl group has been used as a protecting group to prevent Deils–Alder reactions between alkynes and cyclopentadienone-type dienes,[340] it was speculated that the high

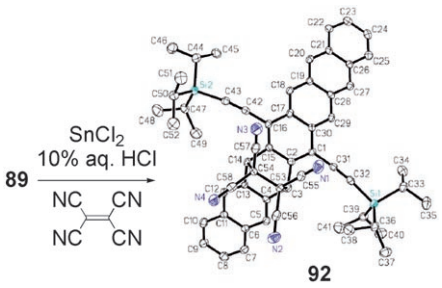

Scheme 14. Trapping reactive heptacene **92** with TCNE.

diene reactivity of the larger acenes necessitates the use of even bulkier substituents to protect the alkyne. Recent reports of Diels–Alder reactions between TIPS-substituted alkynes and heteroheptacene derivatives further supported this conclusion (TIPS = triisopropylsilyl).[341] Increasing the size of the alkyne substituent to tri(*tert*-butylsilyl) (TTBS) yielded a stable, soluble hexacene derivative (**93**; Scheme 15).

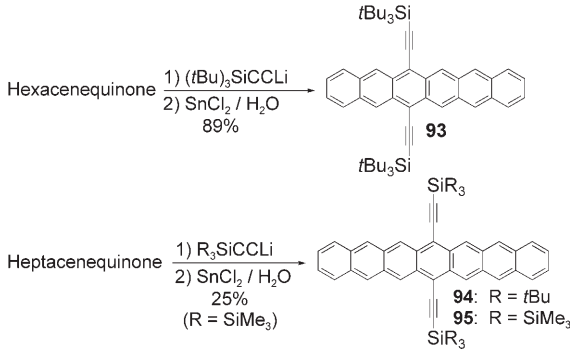

Scheme 15. Syntheses of stable, soluble derivatives of hexacene and heptacene.

The use of the same alkyne to prepare heptacene **94** led to a fleetingly stable compound, which could only be characterized by UV/Vis spectroscopy and mass spectrometry. Further increasing the size of the alkyne functional group to tris(trimethylsilyl)silyl (TTMSS) finally yielded stable, soluble, heptacene derivative **95**. Hexacene **93** formed deep green, cube-shaped crystals that were stable in air for several months, whereas heptacene **95** formed pale, yellow-green plates that decomposed slowly over several weeks.[337]

The long-wavelength absorption bands of acenes **93–95** show the characteristic acene fine structure (Figure 28). The low-energy absorptions of both heptacene derivatives show a broadening of the fine structure with two overlapping transitions apparent between 800 and 850 nm (exemplified in the absorption spectrum of **94**, Figure 28). A similar phenomenon has been observed in the UV/Vis spectrum of the recently reported parent heptacene **81** (Figure 27). This loss of fine structure has been postulated to arise from a Peierls distortion of the aromatic backbone at this long oligomer length.[342] Alternatively, the large aromatic surface of heptacene may lead to strong aggregation of the materials to yield absorptions from this aggregate form; a similar

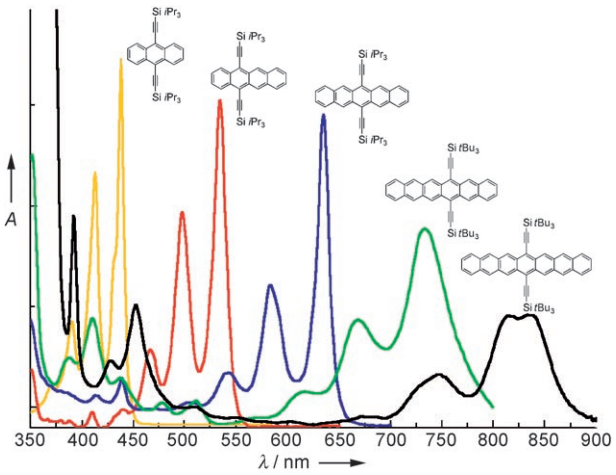

Figure 28. Absorption spectra of functionalized acenes.[337]

observation has been made for the seven-ringed dioxolane functionalized pentacenes.[312] Most likely, a subtle interplay of these effects is the cause of the spectral broadening. The synthesis and characterization of further heptacene derivatives will be necessary for a full investigation of these absorption phenomena.

Absorption spectra for the homologous series of functionalized acenes correlate well with those determined for the parent hydrocarbons. The longest-wavelength absorption values for the silylethyne derivatives from anthracene to heptacene (λ_{max} = 438 nm, 535 nm, 635 nm, 733 nm, and 835 nm, respectively) show a red shift of approximetely 60 nm relative to the parent hydrocarbons anthracene to hexacene (λ_{max} = 376 nm, 474 nm, 578 nm, and 676 nm, respectively). The difference between **94** and **81** (λ_{max} = 760 nm) is somewhat larger, likely because the absorption spectrum of **81** was acquired in a polymer matrix. In both cases, the fusion of additional aromatic rings onto the acene core leads to a remarkably regular bathochromic absorption shift (100 nm).

Crystallographic analysis of hexacene **93** and heptacene **95** confirmed their extended, π-conjugated structure. The availability of high quality crystallographic data for a homologous series of acenes allows examination of the effect of acene length on bond length alternation. Libration-corrected bond lengths[343] for silylethyne-functionalized anthracene,[344] tetracene,[86] pentacene,[295] hexacene, and heptacene[337] are provided in Figure 29. Several trends are evident from the structures. The outermost rings of the acene suffer from the most severe bond alternation. In heptacene, some bond lengths approach the values typically seen in nonaromatic conjugated double bonds (1.34 Å). The central ring in these acenes, although it exhibits the least bond alternation, exhibits the longest bonds of the molecule, which is often cited as an indicator of low aromaticity.[345]

A number of theoretical studies on acenes and polyacenes have treated these materials as two linked polyacetylene chains. These studies predict that the bonds separating these chains would elongate as the acene chain grew longer (to

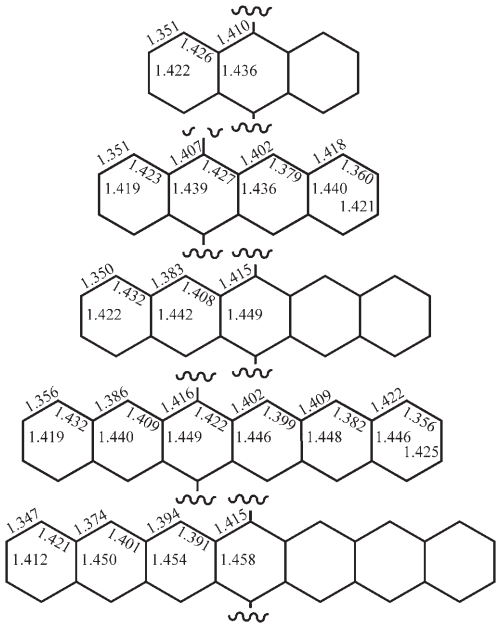

Figure 29. Libration-corrected bond lengths (in Å) for functionalized acences from anthracene to heptacene. The average value is given for all chemically equivalent bond lengths.

reach a final length of 1.46 Å).[346] These predictions are supported by the crystallographic data (Figure 29): the "vertical" bond of the central aromatic ring increases from 1.436 Å (anthracene) to 1.449 Å (pentacene) to 1.458 Å (heptacene). Predictions that bond length alternation decreased toward the center of the acene also appear to be supported by the crystallographic evidence.[347] However, it should be noted that predictions regarding the electronic nature of the parent acenes cannot necessarily be applied to the present materials, since functionalization likely perturbs properties such as ionization energy, singlet/triplet energy gaps,[293] and HOMO–LUMO gaps. Regardless, the availability of a homologous series of materials that can be studied in depth is an important step in the ability to predict the nature of longer acene oligomers and polymeric acene systems.[348]

6. Conclusions and Outlook

Over the last 60 years, painstaking progress was made in understanding electronic processes in organic materials. This progress illuminated the potential of organic semiconductors and provided insight into transport and photophysical properties of organic crystals. The pioneering work of Karl and coworkers in particular emphasized the need for exceptionally high purity to determine intrinsic properties, a requirement that was well understood by researchers in the field of silicon semiconductor technology. Although the research of this period revealed many of the intrinsic properties of smaller acenes, a number of advances were required before acenes could be used in electronic devices such as transistors and solar cells, for example, methods to yield high-purity acene materials and the development of methods to impart appropriate film morphology by thermal evaporation methods. Further improvement and refinement of device fabrication processes led to techniques specifically tailored to the properties of organic semiconductors. Along with the development of vapor transport methods that yielded large, high-quality crystals, it then became possible to fabricate transistor devices on the surface of single crystals, allowing the determination of the intrinsic transport properties of a number of common organic semiconductors. Most of the contemporary problems in organic electronics arise from interactions at interfaces: for example, how to ensure proper morphology of organic compounds grown on inorganic surfaces and how to improve charge transfer between organic semiconductors and metal electrodes. The application of organic materials to electronic devices has moved to a phase at which strong interdisciplinary research will be required to make significant progress.

As the device performance of larger acenes began to match that of amorphous silicon, issues regarding low-cost device fabrication methods gained importance. To allow solution processing, numerous solubilization strategies were developed for these systems, including the addition of removable groups to allow solution deposition and subsequent conversion back into the acene, and the use of permanent functional groups to alter solubility, stability, film morphology, or crystal packing. Both methods yield high-performance transistor devices from solution-cast films, which will allow large-scale device fabrication from low-cost techniques such as screen or ink-jet printing.

Functionalization strategies to improve the processability of pentacene were applied to the synthesis of larger acenes such as heptacene, a molecule that has remained elusive since the controversial reports from Clar and Marschalk in the 1940s. Within the space of one year, both permanent and removable functional groups were used to yield both the parent heptacene and a soluble, crystalline derivative, finally allowing the study of the electronic and structural properties of these unique aromatic materials.

Our understanding of the intrinsic properties of very simple larger acenes is still at an early stage, and new acene derivatives made possible by advances in synthetic chemistry are still being characterized. Although the basic electronic performance of larger acenes such as pentacene approaches that required for commercialization, further work must now be undertaken to address outstanding processing and engineering issues: strategies involving removable functional groups still often require high-temperature annealing, while those using permanent functional groups must address film uniformity issues for the fabrication of large-area devices. And although heretofore elusive heptacenes have finally been prepared and characterized, theoreticians have set nonacene as the point at which the most intriguing properties may be seen—thus providing a new challenge to the synthetic chemists. The resurgence of aromatic chemistry ushered in by the impressive properties of larger acenes will only serve to improve synthetic methods, yield new methods for purification and crystal growth, and further solidify our understanding of this unique class of aromatic materials.

7. Addendum (November 8, 2007)

Since this manuscript was first written progress in the synthesis, characterization, and application of acenes has progressed. Along with the report of the synthesis and device studies of new rubrene derivatives,[349] new syntheses of 2,9,6,13-substituted pentacenes have been reported.[350] Functionalized pentacenes such as **65** have been incorporated into the backbone of conjugated polymers,[351] as well as linked through saturated bridges.[352] Computational studies show the great potential for nitrogen-[353] and nitrile-containing[354] pentacenes as n-type semiconductors. Another report outlined the difficulties involved in the preparation of aryl-substituted hexacenes, and the isolation of hexacene in a polymer matrix.[355]

8. Abbreviations

AFM	atomic force microscopy
Alq_3	tris(quinolin-8-olato)aluminum(III)
DFT	density functional theory
FET	field-effect transistor
FTIR	Fourier transform infrared spectroscopy
HOMO	highest occupied molecular orbital
LCD	liquid-crystal display
LEFET	light-emitting field-effect transistor
LUMO	lowest unoccupied molecular orbital
OLED	organic light-emitting diode
OTS	octadecyltrichlorosilane
PDMS	poly(dimethylsiloxane)
PEDOT/PSS	poly(ethylenedioxythiophene)/poly(styrenesulfonate)
PMMA	poly(methyl methacrylate)
PVA	poly(vinyl alcohol)
PVP	poly(vinyl phenol)
RFID	radio frequency identification
SAM	self-assembled monolayer
SCE	standard calomel electrode
SCLC	space-charge-limited current
STM	scanning tunneling microscopy
TCNE	tetracyanoethylene
TES	triethysilyl
TFT	thin-film transistor
THF	tetrahydrofuran
TIPS	triisopropylsilyl
TOF	time of flight
TTBS	tri-*tert*-butylsilyl
TTMSS	tris(trimethylsilyl)silyl
XRD	X-ray diffraction

This work was supported by the Office of Naval Research and the Advanced Carbon Nanotechnology Program at the University of Kentucky. The author thanks Prof. Tom Jackson, Pennsylvania State University, for providing graphics for the frontispiece of this article, and Dr. Sean Parkin, University of Kentucky, for helpful discussions on pentacene polymorphism.

Received: October 2, 2006
Published online: November 28, 2007

[1] Y. Ruiz-Morales, *J. Phys. Chem. A* **2002**, *106*, 11283.
[2] N. Karl in *Crystals, Growth, Properties and Applications*, *Vol. 4* (Ed.: H. C. Freyhardt), Springer, Berlin, **1980**.
[3] W. Warta, N. Karl, *Phys. Rev. B* **1985**, *32*, 1172.
[4] N. Karl, *Chem. Scr.* **1981**, *17*, 201.
[5] For a recent review of transport measurements, see: N. Karl, *Synth. Met.* **2003**, *133*, 649.
[6] W.-Q. Deng, W. A. Goddard III, *J. Phys. Chem. B* **2004**, *108*, 8614.
[7] a) Y. C. Cheng, R. J. Silbey, D. A. da Silva Filho, J. P. Calbert, J. Cornil, J. L. Brédas, *J. Chem. Phys.* **2003**, *118*, 3764; b) K. Hannewald, P. A. Bobbert, *AIP Conf. Proc.* **2005**, *772*, 1101.
[8] G. Brocks, J. van den Bring, A. Morpurgo, *Phys. Rev. Lett.* **2004**, *93*, 146405.
[9] K. Hummer, C. Ambrosch-Draxl, *Phys. Rev. B* **2005**, *71*, 081202; see also: J. L. Brédas, D. Beljonne, V. Coropceanu, J. Cornil, *Chem. Rev.* **2004**, *104*, 4971.
[10] E. Clar, *Polycyclic Hydrocarbons*, *Vol. 1*, Academic Press, New York, **1964**.
[11] J. H. Schön, C. Kloc, A. Dodabalapur, B. Batlogg, *Science* **2000**, *289*, 599.
[12] J. H. Schön, C. Kloc, B. Batlogg, *Nature* **2000**, *406*, 702.
[13] J. H. Schön, S. Berg, C. Kloc, B. Batlogg, *Science* **2000**, *287*, 1022.
[14] M. R. Beasley, S. Datta, H. Kogelnik, H. Kroemer, D. Monroe. *Report of the Investigation Committee on the Possibility of Scientific Misconduct in the Work of Hendrik Schön and Coauthors.* http://publish.aps.org/reports/ (DOI: 10.1103/aps.reports.lucent). Lucent Technologies/American Physical Society, September 2002.
[15] For a partial list of retracted articles, see: a) *Science* **2002**, *298*, 961; b) *Nature* **2003**, *422*, 93.
[16] For recent coverage of this topic, see: *Printed Organic and Molecular Electronics* (Eds.: D. Gamota, P. Brazis, K. Kalyanasundaram, J. Zhang), Springer, Berlin, **2005**.
[17] H. Sirringhaus, *Adv. Mater.* **2005**, *17*, 2411.
[18] For a recent review, see: A. Facchetti, *Mater. Today* **2007**, *10*, 28; see also: a) F. Würthner, R. Schmidt, *ChemPhysChem* **2006**, *7*, 793; b) G. Witte, C. Wöll, *J. Mater. Res.* **2004**, *19*, 1889; c) C. Ziegler, D. Fichou *Handbook of Oligo- and Polythiophenes* (Ed.: D. Fichou), Wiley-VCH, Weinheim, **1999**, pp. 183–282.
[19] For reviews of the many proposed uses of organic electronics, see: a) T. W. Kelley, P. F. Baude, C. Gerlach, D. E. Ender, D. Muyres, D. Haase, D. E. Vogel, S. D. Theiss, *Chem. Mater.* **2004**, *16*, 4413; b) H. E. Katz, *Chem. Mater.* **2004**, *16*, 4748; c) S. R. Forrest, *Nature* **2004**, *428*, 911.
[20] F. Liao, C. Chen, V. Subramanian, *Sens. Actuators B* **2005**, *107*, 849.
[21] G. Li, V. Shrotriya, I. Huang, Y. Yao, T. Moriarty, K. Emery, Y. Yang, *Nat. Mater.* **2005**, *4*, 864.
[22] C. W. Tang, S. A. VanSlyke, *Appl. Phys. Lett.* **1987**, *51*, 913; For a review: N. K. Patel, S. Cina, J. H. Burroughes, *IEEE J. Sel. Top. Quantum Electron.* **2002**, *8*, 346.
[23] For microwave studies on pentacene, see: A. Saeki, S. Seki, S. Tagawa, *J. Appl. Phys.* **2006**, *100*, 023703; for a review of this technique, see: J. M. Warman, M. P. de Haas, G. Dicker, F. G. Grozema, J. Piris, M. G. Debije, *Chem. Mater.* **2004**, *16*, 4600.
[24] M. C. Beard, G. M. Turner, C. A. Schmuttenmaer, *Phys. Rev. B* **2000**, *62*, 15764.
[25] W. Warta, R. Stehle, N. Karl, *Appl. Phys. A* **1985**, *36*, 163.
[26] D. C. Hoesterey, G. M. Letson, *J. Phys. Chem. Solids* **1963**, *24*, 1609.
[27] M. Campos, *Mol. Cryst. Liq. Cryst.* **1972**, *18*, 105.
[28] a) A. Geurst, *Phys. Status Solidi* **1966**, *15*, 107; R. Zuleeg, P. Knoll, *Appl. Phys. Lett.* **1967**, *11*, 183; b) O. D. Jurchescu, T. T. M. Palstra, *Appl. Phys. Lett.* **2006**, *88*, 122101.

[29] M. A. Lampert, P. Mark, *Current Injection in Solids* (Eds.: H. G. Booker, N. DeClaris), Academic Press, New York, **1970**.
[30] a) P. N. Murgatroyd, *J. Phys. D* **1970**, *3*, 151; b) P. W. M. Blom, M. J. M. de Jong, J. J. M. Vleggaar, *Appl. Phys. Lett.* **1996**, *68*, 3308; c) S. Nespurek, J. Sworakowski, *J. Appl. Phys.* **1980**, *51*, 2098; d) F. Schauer, S. Nespurek, H. Valerìan, *J. Appl. Phys.* **1996**, *80*, 880.
[31] R. W. I. de Boer, M. Jochemsen, T. M. Klapwijk, A. F. Morpurgo, J. Niemax, A. K. Tripathi, J. Pflaum, *J. Appl. Phys.* **2004**, *95*, 1196.
[32] J. R. Sheats, *J. Mater. Res.* **2004**, *19*, 1974.
[33] M. Bendikov, F. Wudl, D. F. Perepichka, *Chem. Rev.* **2004**, *104*, 4891.
[34] J. E. Anthony, *Chem. Rev.* **2006**, *106*, 5028.
[35] K. Wiberg, *J. Org. Chem.* **1997**, *62*, 5720.
[36] J. D. Cox, G. Pilcher, *Thermochemistry of Organic and Organometallic Compounds*, Academic Press, New York, **1970**.
[37] S. A. Odom, S. R. Parkin, J. E. Anthony, *Org. Lett.* **2003**, *5*, 4245.
[38] J. M. Robertson, V. C. Sinclair, J. Trotter, *Acta Cryst.* **1961**, *14*, 697.52.
[39] P. B. Maciejczyk, J. H. Offenberg, J. Clemente, M. Blaustein, G. D. Thurston, L. C. Chen, *Atmos. Environ.* **2004**, *38*, 5283.
[40] Y. A. Elhassaneen, *Nutrition Res.* **2004**, *24*, 435.
[41] a) J. Fritzche, *C. R. Hebd. Seances Acad. Sci.* **1867**, *69*, 1035; b) H. Bouas-Laurent, H. Dürr, *Pure Appl. Chem.* **2001**, *73*, 639.
[42] a) J. J. Schneider, D. Wolf, C. W. Lehmann, *Inorg. Chim. Acta* **2003**, *350*, 625; b) T. Murahashi, M. Fujimoto, M.-a. Oka, Y. Hashimoto, T. Uemura, Y. Tatsumi, Y. Nakao, A. Ikeda, S. Sakaki, H. Kurosawa, *Science* **2006**, *313*, 1104.
[43] T. Takenobu, T. Takano, M. Shiraishi, Y. Murakami, M. Ata, H. Kataura, Y. Achiba, Y. Iwasa, *Nat. Mater.* **2003**, *2*, 683.
[44] Z. Rang, A. Haraldsson, D. M. Kim, P. P. Ruden, R. J. Chesterfield, C. D. Frisbie, *Appl. Phys. Lett.* **2001**, *79*, 2731.
[45] I. Shirotani, Y. Kamura, H. Inokuchi, *Mol. Cryst. Liq. Cryst.* **1974**, *28*, 345.
[46] A. M. Pivovar, J. E. Curtis, J. B. Leao, R. J. Chesterfield, C. D. Frisbie, *Chem. Phys.* **2006**, *325*, 138.
[47] J. Kalinowski, J. Godlewski, R. Jankowiak, *Chem. Phys. Lett.* **1976**, *43*, 127.
[48] E. Venuti, R. G. Della Valle, L. Farina, A. Brillante, M. Masino, A. Girlando, *Phys. Rev. B* **2004**, *70*, 104106.
[49] For a recent review of single-crystal studies, see: C. Reese, Z. Bao, *J. Mater. Chem.* **2006**, *16*, 329.
[50] N. Karl, *Crystals, Growth, Properties and Applications*, *Vol. 4* (Ed. H. C. Freyhardt), Springer, Berlin, **1980**, pp. 1 – 100.
[51] a) C. Kloc, P. G. Simpkins, T. Siegrist, R. A. Laudise, *J. Cryst. Growth* **1997**, *182*, 416; b) R. A. Laudise, C. Kloc, P. G. Simpkins, T. Siegrist, *J. Cryst. Growth* **1998**, *187*, 449.
[52] For a detailed review of crystal growth and device study, see: R. W. I. de Boer, M. E. Gershenson, A. F. Morpurgo, V. Podzorov, *Phys. Status Solidi A* **2004**, *201*, 1302.
[53] G. Goldmann, S. Haas, C. Krellner, K. P. Pernstich, D. J. Gundlach B. Batlogg, *J. Appl. Phys.* **2004**, *96*, 2080.
[54] J. Pflaum, J. Niemax, A. K. Tripathy, *Chem. Phys.* **2006**, *325*, 152.
[55] N. Karl, K.-H. Kraft, J. Marktanner, M. Münch, F. Schatz, R. Stehle, H.-M. Uhde, *J. Vac. Sci. Technol. A* **1999**, *17*, 2318.
[56] R. W. I. de Boer, M. Jochemsen, T. M. Klapwijk, A. F. Morpurgo, J. Niemax, A. K. Tripathi, J. Pflaum, *J. Appl. Phys.* **2004**, *95*, 1196.
[57] a) R. W. I. de Boer, A. F. Morpurgo, *Phys. Rev. B* **2005**, *72*, 073207; b) J. Reynaert, K. Poot, V. Arkhipov, G. Borghs, P. Heremans, *J. Appl. Phys.* **2005**, *97*, 063711.
[58] a) J. Reynaert, V. I. Arkhipov, G. Borghs, P. Heremans, *Appl. Phys. Lett.* **2004**, *85*, 603; b) V. I. Arkhipov, E. V. Emelianova, Y. H. Tak, H. Bassler, *J. Appl. Phys.* **1998**, *84*, 848.
[59] U. Sondermann, A. Kutoglu, H. Bässler, *J. Phys. Chem.* **1985**, *89*, 1735.
[60] V. Podzorov, V. M. Pudalov, M. E. Gershenson, *Appl. Phys. Lett.* **2003**, *82*, 1739.
[61] V. Podzorov, S. E. Sysoev, E. Loginova, V. M. Pudalov, M. E. Gershenson, *Appl. Phys. Lett.* **2003**, *83*, 3504.
[62] a) R. W. I. de Boer, T. M. Klapwijk, A. F. Morpurgo, *Appl. Phys. Lett.* **2003**, *83*, 4345; b) C. R. Newman, R. J. Chesterfield, J. A. Merlo, C. D. Frisbie, *Appl. Phys. Lett.* **2004**, *85*, 422.
[63] D. J. Gundlach, L.-L. Jia, T. N. Jackson, *IEEE Electron Device Lett.* **2001**, *22*, 571.
[64] J. Takeya, T. Nishikawa, T. Takenobu, S. Kobayashi, Y. Iwasa, T. Mitani, C. Goldmann, C. Krellner, B. Batlogg, *Appl. Phys. Lett.* **2004**, *85*, 5078.
[65] a) A. R. Völkel, R. A. Street, D. Knipp, *Phys. Rev. B* **2002**, *66*, 195336; b) K. P. Pernstich, S. Haas, D. Oberhoff, C. Goldmann, D. J. Gundlach, B. Batlogg, A. N. Rashid, G. Schitter, *J. Appl. Phys.* **2004**, *96*, 6431; c) K. P. Pernstich, C. Goldmann, C. Krellner, D. Oberhoff, D. J. Gundlach, B. Batlogg, *Synth. Met.* **2004**, *146*, 325.
[66] a) M. J. Panzer, C. D. Frisbie, *Appl. Phys. Lett.* **2006**, *88*, 203504; b) J. Takeya, K. Yamada, K. Hara, K. Shigeto, K. Tsukagoshi, S. Ikehata, Y. Aoyagi, *Appl. Phys. Lett.* **2006**, *88*, 112102.
[67] R. Zeis, C. Besnard, T. Siegrist, C. Schlockerman, Z. Chi, C. Kloc, *Chem. Mater.* **2006**, *18*, 244.
[68] D. A. da Silva Filho, E.-G. Kim, J.-L. Brédas, *Adv. Mater.* **2005**, *17*, 1072.
[69] a) V. Podzorov, E. Menard, A. Borissov, V. Kiryukhin, J. A. Rogers, M. E. Gershenson, *Phys. Rev. Lett.* **2004**, *93*, 086602; b) E. Menard, V. Podzorov, S.-H. Hur, A. Gaur, M. E. Gershenson, J. A. Rogers, *Adv. Mater.* **2004**, *16*, 2097.
[70] a) D. E. Henn, W. G. Williams, *J. Appl. Crystallogr.* **1971**, *4*, 256; b) W. H. Taylor, *Z. Kristallogr.* **1936**, *93*, 151; c) S. A. Akopyan, R. L. Avoyan, Y. T. Struchkov, *Zh. Strukt. Khim.* **1962**, *3*, 602.
[71] O. D. Jurchescu, A. Meetsma, T. T. M. Palstra, *Acta Crystallogr. Sect. B* **2006**, *62*, 330.
[72] V. C. Sundar, J. Zaumseil, V. Podzorov, E. Menard, R. L. Willett, T. Someya, M. E. Gershenson, J. A. Rogers, *Science* **2004**, *303*, 1644.
[73] V. Podzorov, E. Menard, J. A. Rogers, M. E. Gershenson, *Phys. Rev. Lett.* **2005**, *95*, 226601.
[74] J. Takeya, K. Tsukagoshi, Y. Aoyagi, T. Takenobu, Y. Iwasa, *Jpn. J. Appl. Phys.* **2005**, *44*, 1393.
[75] T. Takahashi, T. Takenobu, J. Takeya, Y. Iwasa, *Appl. Phys. Lett.* **2006**, *88*, 033505.
[76] C. D. Dimitrakopoulos, S. Purushothaman, J. Kymissis, A. Callegari, J. M. Shaw, *Science* **1999**, *283*, 822.
[77] G. Horowitz, X.-Z. Peng, D. Fichou, F. Garnier, *Synth. Met.* **1992**, *51*, 419.
[78] D. J. Gundlach, J. A. Nichols, L. Zhou, T. N. Jackson, *Appl. Phys. Lett.* **2002**, *80*, 2925.
[79] C. Cicoira, F. Santato, F. Dinelli, R. Biscarini, M. Zamboni, M. Muccini, P. Heremans, *Adv. Funct. Mater.* **2005**, *15*, 375.
[80] G. H. Sarova, M. N. Berban-Santos, *Chem. Phys. Lett.* **2004**, *397*, 402.
[81] S. Taillemite, D. Fichou, *Eur. J. Org. Chem.* **2004**, 4981.
[82] C.-W. Chu, Y. Shao, V. Shrotriya, Y. Yang, *Appl. Phys. Lett.* **2005**, *86*, 243506.
[83] A. Hepp, H. Heil, W. Weise, M. Ahles, R. Schmechel, H. von Seggern, *Phys. Rev. Lett.* **2003**, *91*, 157406.
[84] S. L. Murov, I. Carmichael, G. L. Hug *Handbook of Photochemistry*, 2nd ed., Marcel Dekker, New York, **1993**.
[85] R. W. T. Higgins, A. P. Monkman, H.-G. Nothofer, U. Scherf, *Appl. Phys. Lett.* **2001**, *79*, 857.
[86] S. A. Odom, S. R. Parkin, J. E. Anthony, *Org. Lett.* **2003**, *5*, 4245.

[87] J. Reichwagen, H. Hopf, A. Del Guerzo, J.-P. Desvergne, H. Bouas-Laurent, *Org. Lett.* **2004**, *6*, 1899.
[88] a) J. Reichwagen, H. Hopf, A. Del Guerzo, C. Belin, H. Bouas-Laurent, J.-P. Desvergne, *Org. Lett.* **2005**, *7*, 971; b) A. Del Guerzo, A. G. L. Olive, J. Reichwagen, H. Hopf, J.-P. Desvergne, *J. Am. Chem. Soc.* **2005**, *127*, 17984.
[89] a) J. Reichwagen, H. Hopf, J.-P. Desvergne, A. Del Guerzo, H. Bouas-Laurent, *Synthesis* **2005**, 3505; b) J.-P. Desvergne, A. Del Guerzo, H. Bouas-Laurent, C. Belin, J. Reichwagen, H. Hopf, *Pure Appl. Chem.* **2006**, *78*, 707.
[90] G. S. Tulevski, Q. Miao, M. Fukuto, R. Abram, B. Ocko, R. Pindak, M. L. Steigerwald, C. R. Kagan, C. Nuckolls, *J. Am. Chem. Soc.* **2004**, *126*, 15048.
[91] H. Moon, R. Zeis, E.-J. Borkent, C. Besnard, A. J. Lovinger, T. Siegrist, C. Kloc, Z. Bao, *J. Am. Chem. Soc.* **2004**, *126*, 15322.
[92] Z. Chen, P. Müller, T. M. Swager, *Org. Lett.* **2006**, *8*, 273.
[93] Q. Miao, M. Lefenfeld, T.-Q. Nguyen, T. Siegrist, C. Kloc, C. Nuckolls, *Adv. Mater.* **2005**, *17*, 407.
[94] A. M. Müller, Y. S. Avlasevich, K. Müllen, C. J. Bardeen, *Chem. Phys. Lett.* **2006**, *421*, 518.
[95] a) J. A. Merlo, C. R. Newman, C. P. Gerlach, T. W. Kelley, D. V. Muyres, S. Fritz, M. F. Toney, C. D. Frisbie, *J. Am. Chem. Soc.* **2005**, *127*, 3997; b) M. Roth, M. Rehahn, M. Ahles, R. Schmechel, H. von Seggern, *Mater. Res. Soc. Symp. Proc.* **2005**, *871E*, I6.29.1-6. See also M. Rehahn, M. Roth, H. von Seggern, R. Schmechel, M. Ahles, Patent WO/2007/000268, **2007**.
[96] a) S. Kowarik, A. Gerlach, S. Sellner, F. Schreiber, J. Pflaum, L. Cavalcanti, O. Konovalov, *Phys. Chem. Chem. Phys.* **2006**, *8*, 1834; b) D. Käfer, L. Ruppel, G. Witte, C. Wöll, *Phys. Rev. Lett.* **2005**, *95*, 166602.
[97] N. Stingelin-Stutzmann, E. Smits, H. Wondergem, C. Tanase, P. Plom, P. Smith, D. De Leeuw, *Nat. Mater.* **2005**, *4*, 601.
[98] A. L. Briseno, S. C. B. Mannsfeld, M. M. Ling, S. Liu, R. J. Tseng, C. Reese, M. E. Roberts, Y. Yang, F. Wudl, Z. Bao, *Nature* **2006**, *444*, 913.
[99] J. B. Birks, *Photophysics of Aromatic Molecules*, Wiley-Interscience, New York, **1970**.
[100] N. Niiegorodov, D. P. Winkoup, *Spectrochim. Acta Part A* **1997**, *53*, 2013.
[101] H.-H. Perkampus, I. Sandeman, C. J. Timmons, *DMS UV Atlas of Organic Compounds*, Verlag Chemie, Weinheim, **1971**.
[102] a) W. E. Moerner, L. Kador, *Phys. Rev. Lett.* **1989**, *62*, 2535; b) M. Orrit, J. Bernard, *Phys. Rev. Lett.* **1990**, *65*, 2716; c) W. P. Ambrose, W. E. Moerner, *Nature* **1991**, *349*, 225.
[103] a) Y. Durand, A. Bloeß, A. M. van Oijen, J. Köhler, E. J. J. Groenen, J. Schmidt, *Chem. Phys. Lett.* **2000**, *317*, 232; b) J. Köhler, J. A. J. M. Disselhorst, M. C. J. M. Donckers, E. J. J. Groenen, J. Schmidt, W. E. Moerner, *Nature* **1993**, *363*, 242; c) J.-L. Ong, D. J. Sloop, T.-S. Lin, *J. Phys. Chem.* **1993**, *97*, 7833.
[104] R. B. Campbell, J. M. Robertson, J. Trotter, *Acta Crystallogr.* **1961**, *14*, 705.
[105] R. B. Campbell, J. M. Robertson, J. Trotter, *Acta Crystallogr.* **1962**, *15*, 289.
[106] a) D. Holmes, S. Kumaraswamy, A. J. Matzger, K. P. C. Vollhardt, *Eur. J. Org. Chem.* **1999**, 3399; b) C. C. Mattheus, A. B. Dros, J. Baas, A. Meetsma, J. L. de Boer, T. T. M. Palstra, *Acta Crystallogr. Sect. C* **2001**, *57*, 939.
[107] a) E. Venuti, R. G. Della Valle, A. Brillante, M. Masino, A. Girlando, *J. Am. Chem. Soc.* **2002**, *124*, 2128; b) R. G. Della Valle, E. Venuti, A. Brillante, A. Girlando, *J. Chem. Phys.* **2003**, *118*, 807.
[108] a) L. Farina, A. Brillante, R. G. Della Valle, E. Venuti, M. Amboage, K. Syassen, *Chem. Phys. Lett.* **2003**, *375*, 490; b) R. G. Della Valle, A. Brillante, L. Farina, E. Venuti, M. Masino, A. Girlando, *Mol. Cryst. Liq. Cryst.* **2004**, *416*, 145.
[109] R. A. Hawley-Fedder, M. L. Parsons, F. W. Karasek, *J. Chromat.* **1987**, *387*, 207.
[110] M. S. De Vries, K. Reihs, H. R. Wendt, W. G. Golden, H. E. Hunziker, R. Fleming, E. Peterson, S. Chang, *Geochim. Cosmochim. Acta* **1993**, *57*, 933.
[111] W. Reid, F. Anthöfer, *Angew. Chem.* **1954**, *66*, 604.
[112] E. P. Goodings, D. A. Mitchard, G. Owen, *J. Chem. Soc. Perkin Trans. 1* **1972**, 1310.
[113] J. G. Laquindanum, H. E. Katz, A. J. Lovinger, *J. Am. Chem. Soc.* **1998**, *120*, 664.
[114] T. Minakata, Y. Natsume, *Synth. Met.* **2005**, *153*, 1.
[115] A. R. Reddy, M. Bendikov, *Chem. Commun.* **2006**, 1179.
[116] O. Berg, E. L. Chronister, T. Yamashita, G. W. Scott, R. M. Sweet, J. Calabrese, *J. Phys. Chem. A* **1999**, *103*, 2451.
[117] G. P. Miller, J. Briggs, J. Mack, P. A. Lord, M. M. Olmstead, A. L. Balch, *Org. Lett.* **2003**, *5*, 4199.
[118] R. A. B. Devine, M.-M. Ling, A. B. Mallik, M. Roberts, Z. Bao, *Appl. Phys. Lett.* **2006**, *88*, 151907.
[119] V. I. Arkhipov, V. A. Kolesnikov, A. I. Rudenko, *J. Phys. D* **1984**, *17*, 1241.
[120] J. Cornil, J. Ph. Calbert, J. L. Brédas, *J. Am. Chem. Soc.* **2001**, *123*, 1250.
[121] N. E. Gruhn, D. A. da Silva Filho, T. G. Bill, M. Malagoli, V. Coropceanu, A. Kahn, J.-L. Brédas, *J. Am. Chem. Soc.* **2002**, *124*, 7918.
[122] Y. Olivier, V. Lemaur, J. L. Brédas, J. Cornil, *J. Phys. Chem. A* **2006**, *110*, 6356.
[123] J. L. Brédas, J. P. Calbert, D. A. da Silva Filho, J. Cornil, *Proc. Natl. Acad. Sci. USA* **2002**, *99*, 5804.
[124] A. Troisi, G. Orlandi, *J. Phys. Chem. B* **2005**, *109*, 1849.
[125] A. Troisi, G. Orlandi, *J. Phys. Chem. A* **2006**, *110*, 4065.
[126] T. Minakata, I. Nagoya, M. Ozaki, *J. Appl. Phys.* **1991**, *69*, 7354.
[127] T. Ito, T. Mitani, T. Takenobu, Y. Iwasa, *J. Phys. Chem. Solids* **2004**, *65*, 609.
[128] B. Fang, H. Zhou, I. Honma, *Appl. Phys. Lett.* **2005**, *86*, 261909.
[129] a) B. Fang, H. Zhou, I. Honma, *J. Chem. Phys.* **2006**, *124*, 204718; b) B. Fang, H. Zhou, I. Honma, *Appl. Phys. Lett.* **2006**, *89*, 023102.
[130] A. Brillante, J. Bilotti, R. G. Della Valle, E. Venuti, M. Masino, A. Girlando, *Adv. Mater.* **2005**, *17*, 2549.
[131] J. Takeya, C. Goldmann, S. Haas, K. P. Pernstich, B. Ketterer, B. Batlogg, *J. Appl. Phys.* **2003**, *94*, 5800.
[132] V. Y. Butko, X. Chi, D. V. Lang, A. P. Ramirez, *Appl. Phys. Lett.* **2003**, *83*, 4773.
[133] R. He, X. Chi, A. Pinczuk, D. V. Lang, A. P. Ramirez, *Appl. Phys. Lett.* **2005**, *87*, 211117.
[134] L. B. Roberson, J. Kowalik, L. M. Tolbert, C. Kloc, R. Zeis, X. Chi, R. Fleming, C. Wilkins, *J. Am. Chem. Soc.* **2005**, *127*, 3069.
[135] C. C. Mattheus, J. Baas, A. Meersma, J. L. de Boer, C. Kloc, T. Siegrist, T. T. M. Palstra, *Acta Crystallogr. Sect. E* **2002**, *58*, 1229.
[136] O. D. Jurchescu, M. Popinciuc, B. J. van Wees, T. T. M. Palstra, *Adv. Mater.* **2007**, *19*, 688.
[137] O. D. Jurchescu J. Baas, T. T. M. Palstra, *Appl. Phys. Lett.* **2004**, *84*, 3061.
[138] O. D. Jurchescu, T. T. M. Palstra, *Appl. Phys. Lett.* **2006**, *88*, 122101.
[139] J. Y. Lee, S. Roth, Y. W. Park, *Appl. Phys. Lett.* **2006**, *88*, 252106.
[140] G. A. de Wijs, C. C. Mattheus, R. A. de Groot, T. T. M. Palstra, *Synth. Met.* **2003**, *139*, 109.
[141] C. Goldmann, D. J. Gundlach, B. Batlogg, *Appl. Phys. Lett.* **2006**, *88*, 063501.
[142] O. D. Jurchescu, J. Baas, T. T. M. Palstra, *Appl. Phys. Lett.* **2005**, *87*, 052102.
[143] For recent reviews of organic transistors and devices, see: a) G. Horowitz, *J. Mater. Res.* **2004**, *19*, 1946; b) C. R. Newman, C. D. Frisbie, D. A. da Silva Filho, J.-L. Brédas, P. C. Ewbank, K. R.

Mann, *Chem. Mater.* **2004**, *16*, 4436; c) Z. Bao, *Adv. Mater.* **2000**, *12*, 227.
[144] C. D. Dimitrakopoulos, P. R. L. Malenfant, *Adv. Mater.* **2002**, *14*, 99.
[145] a) G. Horowitz, D. Fichou, X. Peng, F. Garnier, *Synth. Met.* **1991**, *41*, 1127; b) G. Horowitz, X. Z. Peng, D. Fichou, F. Garnier, *Synth. Met.* **1992**, *51*, 419.
[146] a) C. D. Dimitrakopoulos, A. R. Brown, A. Pomp, *J. Appl. Phys.* **1996**, *80*, 2501; b) Y. Lin, D. J. Gundlach, T. N. Jackson, *Ann. Dev. Res. Conf. Dig.* **1996**, 80.
[147] Y. Y. Lin, D. J. Gundlach, S. Nelson, T. N. Jackson, *IEEE Trans. Electron Devices* **1997**, *44*, 1325.
[148] S. F. Nelson, Y.-Y. Lin, D. J. Gundlach, T. N. Jackson, *Appl. Phys. Lett.* **1998**, *72*, 1854.
[149] I. Kymissis, C. D. Dimitrakopoulos, S. Purushothaman, *IEEE Trans. Electron Devices* **2001**, *48*, 1060.
[150] P. V. Pesavento, R. J. Chesterfield, C. R. Newman, C. D. Frisbie, *J. Appl. Phys.* **2004**, *96*, 7312.
[151] C. R. Newman, R. J. Chesterfield, M. J. Panzer, C. D. Frisbie, *J. Appl. Phys.* **2005**, *98*, 084506.
[152] M.-M. Ling, Z. Bao, D. Li, *Appl. Phys. Lett.* **2006**, *88*, 033502.
[153] T. Sekitani, Y. Takamatsu, S. Nakano, T. Sakurai, T. Someya, *Appl. Phys. Lett.* **2006**, *88*, 253508.
[154] J. G. Laquindanum, H. E. Katz, A. J. Lovinger, A. Dodabalapur, *Chem. Mater.* **1996**, *8*, 2542.
[155] R. Ruiz, D. Choudhary, B. Nickel, T. Toccoli, K-C. Chang, A. C. Mayer, P. Clancy, J. M. Blakely, R. L. Headrick, S. Iannotta, G. G. Malliaras, *Chem. Mater.* **2004**, *16*, 4497.
[156] a) I. P. M. Bouchoms, W. A. Schoonveld, J. Vrjmoeth, T. M. Klapwijk, *Synth. Met.* **1999**, *104*, 175; b) C. C. Mattheus, A. B. Dros, J. Baas, G. T. Oostergetel, A. Meetsma, J. L. de Boer, T. T. M. Palstra, *Synth. Met.* **2003**, *138*, 475.
[157] D. J. Gundlach, T. N. Jackson, D. G. Schlom, S. F. Nelson, *Appl. Phys. Lett.* **1999**, *74*, 3302.
[158] C. C. Mattheus, G. A. de Wijs, R. A. de Groot, T. T. M. Palstra, *J. Am. Chem. Soc.* **2003**, *125*, 6323.
[159] a) K. O. Lee, T. T. Gan, *Chem. Phys. Lett.* **1977**, *51*, 120; b) R. Eiermann, G. M. Parkinson, H. Baessler, J. M. Thomas, *J. Phys. Chem.* **1983**, *87*, 544.
[160] A. C. Mayer, R. Ruiz, H. Zhou, R. L. Headrick, A. Kazimirov, G. G. Malliaras, *Phys. Rev. B* **2006**, *73*, 205307.
[161] A. C. Mayer, R. Ruiz, R. L. Headrick, A. Kasimirov, G. G. Malliaras, *Org. Electron.* **2004**, *5*, 257.
[162] S. E. Fritz, S. M. Martin, C. D. Frisbie, M. D. Ward, M. F. Toney, *J. Am. Chem. Soc.* **2004**, *126*, 4084.
[163] H. Yang, T. J. Shin, M.-M. Ling, K. Cho, C. Y. Ryu, Z. Bao, *J. Am. Chem. Soc.* **2005**, *127*, 11542.
[164] a) R. Ruiz, A. Papadimitratos, A. C. Mayer, G. G. Malliaras, *Adv. Mater.* **2005**, *17*, 1795; b) S. Jung, Z. Yao, *Appl. Phys. Lett.* **2005**, *86*, 083505.
[165] L. F. Drummy, P. K. Miska, D. Alberts, N. Lee, D. C. Martin, *J. Phys. Chem. B* **2006**, *110*, 6066.
[166] a) J. H. Kang, X.-Y. Zhu, *Appl. Phys. Lett.* **2003**, *82*, 3248; b) G. E. Thayer, J. T. Sadowski, F. M. zu Herringdorf, T. Sakurai, R. M. Tromp, *Phys. Rev. Lett.* **2005**, *95*, 256106.
[167] F.-J. Meyer zu Heringdorf, M. C. Reuter, R. M. Tromp, *Nature* **2001**, *412*, 517.
[168] K. P. Weidkamp, C. A. Hacker, M. P. Schwartz, X. Cao, R. M. Tromp, R. J. Hamers, *J. Phys. Chem. B* **2003**, *107*, 11142.
[169] See, for example: M. Halik, H. Klauk, U. Zschieschang, G. Schmid, C. Dehm, M. Schuetz, S. Maisch, F. Effenberger, M. Brunnbauer, F. Stellacci, *Nature* **2004**, *431*, 963.
[170] a) C. D. Dimitrakopoulos, I. Kymissis, S. Purushothaman, D. A. Neumayer, P. R. Duncombe, R. B. Laibowitz, *Adv. Mater.* **1999**, *11*, 1372; b) C. D. Dimitrakopoulos, S. Purushothaman, J. Kymissis, A. Callegari, J. M. Shaw, *Science* **1999**, *283*, 822.
[171] S. Steudel, S. De Vusser, S. De Jonge, D. Janssen, S. Verlaak, J. Genoe, P. Heremans, *Appl. Phys. Lett.* **2004**, *85*, 4400.
[172] S. Fritz, T. W. Kelly, C. D. Frisbie, *J. Phys. Chem. B* **2005**, *109*, 10574.
[173] Y. Jin, Z. Rang, M. I. Nathan, P. P. Ruden, C. R. Newman, C. D. Frisbie, *Appl. Phys. Lett.* **2004**, *85*, 4406.
[174] a) D. Knipp, R. A. Street, A. Völkel, J. Ho, *J. Appl. Phys.* **2003**, *93*, 347; b) S. Y. Yang, K. Shin, C. E. Park, *Adv. Funct. Mater.* **2005**, *15*, 1806.
[175] J. Veres, S. Ogier, G. Lloyd, D. de Leeuw, *Chem. Mater.* **2004**, *16*, 4543.
[176] K. Shankar, T. N. Jackson, *J. Mater. Res.* **2004**, *19*, 2003.
[177] a) L. A. Majewski, R. Schroeder, M. Grell, P. A. Glarvey, M. L. Turner, *J. Appl. Phys.* **2004**, *96*, 5781; b) G. Horowitz, P. Lang, M. Mottaghi, H. Aubin, *Adv. Funct. Mater.* **2004**, *14*, 1069.
[178] J.-M. Kim, J.-W. Lee, J.-K. Kim, B.-K. Ju, J.-S. Kim, Y.-H. Lee, M.-H. Oh, *Appl. Phys. Lett.* **2004**, *85*, 6368.
[179] K. P. Pernstich, S. Haas, D. Oberhoff, C. Goldmann, D. J. Gundlach, B. Batlogg, A. N. Rashid, G. Schitter, *J. Appl. Phys.* **2004**, *96*, 6431.
[180] R. Schroeder, J. A. Majewski, M. Grell, *Appl. Phys. Lett.* **2004**, *84*, 1004.
[181] M. J. Panzer, C. R. Newman, C. D. Frisbie, *Appl. Phys. Lett.* **2005**, *86*, 103503.
[182] M. J. Panzer, C. D. Frisbie, *J. Am. Chem. Soc.* **2005**, *127*, 6960.
[183] For a review, see: H. Ishii, K. Sugiyama, E. Ito, K. Seki, *Adv. Mater.* **1999**, *11*, 605.
[184] F. Amy, C. Chan, A. Kahn, *Org. Electron.* **2005**, *6*, 85.
[185] P. G. Schroeder, C. B. France, J. B. Park, B. A. Parkinson, *J. Appl. Phys.* **2002**, *91*, 3010.
[186] P. G. Schroeder, C. B. France, J. B. Park, B. A. Parkinson, *J. Phys. Chem. B* **2003**, *107*, 2253.
[187] J. Reynaert, V. I. Arkhipov, G. Borghs, P. Heremans, *Appl. Phys. Lett.* **2004**, *85*, 603.
[188] N. J. Watkins, L. Yan, Y. Gao, *Appl. Phys. Lett.* **2002**, *80*, 4384.
[189] J. Zaumseil, K. W. Baldwin, J. A. Rogers, *J. Appl. Phys.* **2003**, *93*, 6117.
[190] N. Koch, A. Kahn, J. Ghijsen, J.-J. Pireaux, J. Schwartz, R. L. Johnson, A. Elschner, *Appl. Phys. Lett.* **2003**, *82*, 70.
[191] N. Koch, A. Elschner, J. Schwartz, A. Kahn, *Appl. Phys. Lett.* **2003**, *82*, 2281.
[192] D. J. Gundlach, L. Zhou, J. A. Nichols, T. N. Jackson, P. V. Necliudov, M. S. Shur, *J. Appl. Phys.* **2006**, *100*, 024509.
[193] P. V. Pesavento, K. P. Puntambekar, C. D. Frisbie, J. C. McKeen, P. P. Ruden, *J. Appl. Phys.* **2006**, *99*, 094504.
[194] W.-K. Kim, J.-L. Lee, *Appl. Phys. Lett.* **2006**, *88*, 262102.
[195] W. S. Hu, Y. T. Tao, Y. J. Hsu, D. H. Wei, Y. S. Wu, *Langmuir* **2005**, *21*, 2260.
[196] a) N. Koch, A. Eischner, R. L. Johnson, J. P. Rabe, *Appl. Surf. Sci.* **2005**, *244*, 593; b) N. Koch, A. Eischner, J. P. Rabe, R. L. Johnson, *Adv. Mater.* **2005**, *17*, 330.
[197] A. Ulman, *Chem. Rev.* **1996**, *96*, 1533.
[198] D. J. Gundlach, L. Jia, T. N. Jackson, *IEEE Electron Device Lett.* **2001**, *22*, 571.
[199] K. S. Pyo, C. K. Song, *Thin Solid Films* **2005**, *485*, 230.
[200] D. V. Lang, X. Chi, T. Siegrist, A. M. Sergent, A. P. Ramirez, *Phys. Rev. Lett.* **2004**, *93*, 086802.
[201] B. Nickel, R. Barabash, R. Ruiz, N. Koch, A. Kahn, L. C. Feldman, R. F. Haglund, G. Scoles, *Phys. Rev. B* **2004**, *70*, 125401.
[202] a) R. A. Street, D. Knipp, A. R. Völkel, *Appl. Phys. Lett.* **2002**, *80*, 1658; b) A. R. Völkel, R. A. Street, D. Knipp, *Phys. Rev. B* **2002**, *66*, 195336.
[203] E. M. Muller, J. A. Marohn, *Adv. Mater.* **2005**, *17*, 1410.
[204] G. Horowitz, M. E. Hajlaoui, *Adv. Mater.* **2000**, *12*, 1046.
[205] A. Di Carlo, F. Placenza, A. Bolognesi, B. Stadlober, H. Maresch, *Appl. Phys. Lett.* **2005**, *86*, 263501.

[206] K. Puntambekar, J. Dong, G. Haugstad, C. D. Frisbie, *Adv. Funct. Mater.* **2006**, *16*, 879.
[207] D. V. Lang, X. Chi, T. Siegrist, A. M. Sergent, A. P. Ramirez, *Phys. Rev. Lett.* **2004**, *93*, 076601.
[208] D. B. A. Rep, A. F. Morpurgo, W. G. Sloof, T. M. Klapwijk, *J. Appl. Phys.* **2003**, *93*, 2082.
[209] J. H. Kang, D. da Silva Filho, J.-L. Brédas, X.-Y. Zhu, *Appl. Phys. Lett.* **2005**, *86*, 152115.
[210] J. B. Chang, V. Subramanian, *Appl. Phys. Lett.* **2006**, *88*, 233513.
[211] C. Pannemann, T. Dieckmann, U. Hilleringmann, *J. Mater. Res.* **2004**, *19*, 1999.
[212] C. R. Kagan, A. Afzali, T. O. Graham, *Appl. Phys. Lett.* **2005**, *86*, 193505.
[213] A. Vollmer, O. D. Jurchescu, I. Arfaoui, I. Salzmann, T. T. M. Palstra, P. Rudolf, J. Niemax, J. Pflaum, J. P. Rabe, N. Koch, *Eur. Phys. J. E* **2005**, *17*, 339.
[214] S. Ogawa, T. Naijo, Y. Kimura, H. Ishii, M. Niwano, *Appl. Phys. Lett.* **2005**, *86*, 252104.
[215] D. Li, E.-J. Borkant, R. Nortrup, H. Moon, H. Katz, Z. Bao, *Appl. Phys. Lett.* **2005**, *86*, 042105.
[216] T. Jung, A. Dodabalapur, R. Wenz, S. Mohapatra, *Appl. Phys. Lett.* **2005**, *87*, 182109.
[217] Y. C. Cheng, R. J. Silbey, D. A. da Silva Filho, J. P. Calbert, J. Cornil, J. L. Brédas, *J. Chem. Phys.* **2003**, *118*, 3764.
[218] T. Heim, K. Lmimouni, D. Vuillaume, *Nano Lett.* **2004**, *4*, 2145.
[219] E. Kuwahara, Y. Kubozono, T. Hosokawa, T. Nagano, K. Masunari, A. Fujiwara, *Appl. Phys. Lett.* **2004**, *85*, 4765.
[220] a) T. Jung, B. Yoo, L. Wang, A. Dodabalapur, B. A. Jones, A. Facchetti, M. R. Wasielewski, T. J. Marks, *Appl. Phys. Lett.* **2006**, *88*, 183102; b) K. N. N. Unni, A. K. Pandey, S. Alem, J.-M. Nunzi, *Chem. Phys. Lett.* **2006**, *421*, 554.
[221] M. Ahles, R. Schmechel, H. von Seggern, *Appl. Phys. Lett.* **2004**, *85*, 4499.
[222] R. Schmechel, M. Ahles, H. von Seggern, *J. Appl. Phys.* **2005**, *98*, 084511.
[223] M. Ahles, R. Schmechel, H. von Seggern, *Appl. Phys. Lett.* **2005**, *87*, 113505.
[224] L.-L. Chua, J. Zaumseil, J.-F. Chang, E. C.-W. Ou, P. K.-H. Ho, H. Sirringhaus, R. H. Friend, *Nature* **2005**, *434*, 194.
[225] T. B. Singh, F. Meghdadi, S. Günes, N. Marjanovic, G. Horowitz, P. Lang, S. Bauer, N. S. Sariciftci, *Adv. Mater.* **2005**, *17*, 2315.
[226] T. B. Singh, P. Senkarabacak, N. S. Sariciftci, A. Tanda, C. Lackner, R. Hagelauer, G. Horowitz, *Appl. Phys. Lett.* **2006**, *89*, 033512.
[227] F. Eder, H. Klauk, M. Halik, U. Zschieschang, G. Schmid, C. Dehm, *Appl. Phys. Lett.* **2004**, *84*, 2673.
[228] T. Sekitani, S. Iba, Y. Kato, Y. Noguchi, T. Someya, T. Sakurai, *Appl. Phys. Lett.* **2005**, *87*, 173502.
[229] J. B. Lee, V. Subramanian, *IEEE Trans. Electron Devices* **2005**, *52*, 269.
[230] J. Granstrom, H. E. Katz, *J. Mater. Res.* **2004**, *19*, 3540.
[231] J. Zaumseil, T. Someya, Z. Bao, Y.-L. Loo, R. Cirelli, J. A. Rogers, *Appl. Phys. Lett.* **2003**, *82*, 793.
[232] R. Parashkov, E. Becker, T. Riedl, H.-H. Johannes, W. Kowalsky, *Adv. Mater.* **2005**, *17*, 1523.
[233] S. Y. Park, T. Kwon, H. H. Lee, *Adv. Mater.* **2006**, *18*, 1861.
[234] a) M. Halik, H. Klauk, U. Zschieschang, G. Schmid, W. Radlik, W. Weber, *Adv. Mater.* **2002**, *14*, 1717; b) K. S. Lee, G. B. Blanchet, F. Gao, Y.-L. Loo, *Appl. Phys. Lett.* **2005**, *86*, 074102.
[235] Q. Cao, Z.-T. Zhu, M. G. Lemaitre, M.-G. Xia, M. Shim, J. A. Rogers, *Appl. Phys. Lett.* **2006**, *88*, 113511.
[236] a) Y. Zhang, J. R. Petta, S. Ambily, Y. Shen, D. C. Ralph, G. G. Malliaras, *Adv. Mater.* **2003**, *15*, 1632; b) J. B. Lee, P. C. Chang, A. J. Liddle, V. Subramanian, *IEEE Trans. Electron Devices* **2005**, *52*, 1874; c) L. Wang, D. Fine, T. Jung, D. Basu, H. von Seggern, A. Dodabalapur, *Appl. Phys. Lett.* **2004**, *85*, 1772.
[237] X.-Z. Bo, N. G. Tassi, C. Y. Lee, M. S. Strano, C. Nuckolls, G. B. Blanchet, *Appl. Phys. Lett.* **2005**, *87*, 203510.
[238] G. B. Blanchet, X.-Z. Bo, C. Y. Lee, M. S. Strano, C. Nuckolls, *Solid State Commun.* **2005**, *135*, 638.
[239] Y. Abe, T. Hasegawa, Y. Takahashi, T. Yamada, Y. Tokura, *Appl. Phys. Lett.* **2005**, *87*, 153506.
[240] P. S. Abthagir, Y.-G. Ha, E.-A. You, S.-H. Jeong, H.-S. Seo, J.-H. Choi, *J. Phys. Chem. B* **2005**, *109*, 23918.
[241] T. Toccoli, A. Pallaoro, N. Coppede, S. Ianotta, F. De Angelis, L. Mariucci, G. Fortunato, *Appl. Phys. Lett.* **2006**, *88*, 132106.
[242] G. B. Blanchet, C. R. Fincher, I. Malajovich, *J. Appl. Phys.* **2003**, *94*, 6181.
[243] a) T. Toccoli, A. Pallaoro, N. Coppedé, S. Iannotta, F. De Angelis, L. Mariucci, G. Fortunato, *Appl. Phys. Lett.* **2006**, *88*, 132106; b) C. D. Dimitrakopoulos, A. R. Brown, A. Pomp, *J. Appl. Phys.* **1996**, *80*, 2501; c) L. Casalis, M. F. Danisman, B. Nickel, G. Bracco, T. Toccoli, S. Ianotta, G. Scoles, *Phys. Rev. Lett.* **2003**, *90*, 206101.
[244] H. Y. Choi, S. H. Kim, J. Jang, *Adv. Mater.* **2004**, *16*, 732.
[245] a) M. Shtein, P. Peumans, J. B. Banziger, S. R. Forrest, *J. Appl. Phys.* **2004**, *96*, 4500; b) M. Shtein, P. Peumans, J. B. Benziger, S. R. Forrest, *Adv. Mater.* **2004**, *16*, 1615.
[246] D. Tondelier, K. Lmimouni, D. Vuillaume, C. Fery, G. Haas, *Appl. Phys. Lett.* **2004**, *85*, 5763.
[247] K. N. N. Unni, R. de Bettignies, S. Dabos-Seignon, J.-M. Nunzi, *Appl. Phys. Lett.* **2004**, *85*, 1823.
[248] a) S. Steudel, S. De Vusser, K. Myny, M. Lenes, J. Genoe, P. Heremans, *J. Appl. Phys.* **2006**, *99*, 114519; b) P. F. Baude, D. A. Ender, M. A. Haase, T. W. Kelley, D. V. Muyres, S. D. Theiss, *Appl. Phys. Lett.* **2003**, *82*, 3964; c) S. Steudel, K. Myny, V. Arkhipov, C. Deibel, S. De Vusser, J. Genoe, P. Heremans, *Nat. Mater.* **2005**, *4*, 597; d) S. De Vusser, S. Steudel, K. Myny, J. Genoe, P. Heremans, *Appl. Phys. Lett.* **2006**, *88*, 162116; e) R. Rotzoll, S. Mohapatra, V. Olariu, R. Wenz, M. Grigas, K. Dimmler, O. Shchekin, A. Dodabalapur, *Appl. Phys. Lett.* **2006**, *88*, 123502.
[249] D. J. Gundlach, K. P. Pernstich, G. Wilckens, M. Gruter, S. Haas, B. Batlogg, *J. Appl. Phys.* **2005**, *98*, 064502.
[250] a) H. Klauk, M. Halik, U. Zschieschang, F. Eder, G. Schmid, C. Dehm, *Appl. Phys. Lett.* **2003**, *82*, 4175; b) B. Yoo, T. Jung, D. Basu, A. Dodabalapur, B. A. Jones, A. Facchetti, M. R. Wasielewski, T. J. Marks, *Appl. Phys. Lett.* **2006**, *88*, 082104.
[251] a) E. Kuwahara, H. Kusai, T. Nagano, T. Takayanagi, Y. Kubozono, *Chem. Phys. Lett.* **2005**, *413*, 379; b) C. H. Mueller, N. Theofylaktos, F. A. Miranda, A. T. Johnson, N. J. Pinto, *Thin Solid FIlms* **2006**, *496*, 494.
[252] a) Z.-T. Zhu, J. T. Mason, R. Dieckmann, G. G. Malliaras, *Appl. Phys. Lett.* **2002**, *81*, 4643; b) M. C. Tanese, D. Fine, A. Dodabalapur, L. Torsi, *Biosens. Bioelectron.* **2005**, *21*, 782; c) L. Wang, D. Fine, A. Dodabalapur, *Appl. Phys. Lett.* **2004**, *85*, 6386.
[253] Z. Rang, M. I. Nathan, P. P. Ruden, R. Chesterfield, C. D. Frisbie, *Appl. Phys. Lett.* **2004**, *85*, 5760.
[254] G. Darlinski, U. Bottger, R. Waser, H. Klauk, M. Halik, U. Zschieschang, G. Schmid, C. Dehm, *J. Appl. Phys.* **2005**, *97*, 093708.
[255] T. Someya, Y. Kato, T. Sekitani, S. Iba, Y. Noguchi, Y. Murase, H. Kawaguchi, T. Sakurai, *Proc. Natl. Acad. Sci. USA* **2005**, *102*, 12321, and references therein.
[256] K. Itaka, M. Yamashiro, J. Yamaguchi, M. Haemori, S. Yaginuma, Y. Matsumoto, M. Kondo, H. Koinuma, *Adv. Mater.* **2006**, *18*, 1713.
[257] a) Y.-W. Wang, H.-L. Cheng, Y.-K. Wang, T.-H. Hu, J.-C. Ho, C.-C. Lee, T.-F. Lei, C.-F. Yeh, *Thin Solid Films* **2005**, *491*, 305; b) C. D. Sheraw, L. Zhou, J. R. Huang, D. J. Gundlach, T. N. Jackson, M. G. Kane, I. G. Hill, M. S. Hammond, J. Campi,

B. K. Greening, J. Franci, J. West, *Appl. Phys. Lett.* **2002**, *80*, 1088.
[258] a) C.-W. Chu, C.-W. Chen, S.-H. Li, S. H.-E. Wu, Y. Yang, *Appl. Phys. Lett.* **2005**, *86*, 253503; b) M. Kitamura, T. Imada, Y. Arakawa, *Appl. Phys. Lett.* **2003**, *83*, 3410; c) L. Zhou, A. Wanga, S.-C. Wu, J. Sun, S. Park, T. N. Jackson, *Appl. Phys. Lett.* **2006**, *88*, 083502; d) G.-S. Ryu, K.-B. Choe, C.-K. Song, *Thin Solid Films* **2006**, *514*, 302.
[259] G. H. Gelinck, H. E. A. Huitema, E. van Veenendaal, E. Cantatore, L. Schrijnemakers, J. B. P. H. van der Putten, T. C. T. Geuns, M. Beenhakkers, J. B. Giesbers, B.-H. Huisman, E. J. Meijer, E. M. Benito, F. J. Touwslager, A. W. Marsman, B. J. E. van Rens, D. M. de Leeuw, *Nat. Mater.* **2004**, *3*, 106.
[260] A. Corval, C. Kryschi, S. Astilean, H. P. Trommsdorff, *J. Phys. Chem.* **1994**, *98*, 7376.
[261] a) J. Lee, S. S. Kim, K. Kim, J. H. Kim, S. Im, *Appl. Phys. Lett.* **2004**, *84*, 1701; b) L. Sebastian, G. Weiser, H. Baessler, *Chem. Phys.* **1981**, *61*, 125.
[262] S. Yoo, B. Domercq, B. Kippelen, *Appl. Phys. Lett.* **2004**, *85*, 5427.
[263] A. C. Mayer, M. T. Lloyd, D. J. Herman, T. G. Kasen, G. G. Malliaras, *Appl. Phys. Lett.* **2004**, *85*, 6272.
[264] A. K. Pandey, K. N. N. Unni, J.-M. Nunzi, *Thin Solid Films* **2006**, *511*, 529.
[265] a) A. R. Brown, A. Pomp, D. M. de Leeuw, D. B. M. Klaassen, E. E. Havinaga, P. Herwig, K. Müllen, *J. Appl. Phys.* **1996**, *79*, 2136; b) P. T. Herwig, K. Müllen, *Adv. Mater.* **1999**, *11*, 480.
[266] A. Afzali, C. D. Dimitrakopoulos, T. L. Breen, *J. Am. Chem. Soc.* **2002**, *124*, 8812.
[267] A. Afzali, C. D. Dimitrakopoulos, T. O. Graham, *Adv. Mater.* **2003**, *15*, 2066.
[268] K. P. Weidkamp, A. Afzali, R. M. Tromp, R. J. Hamers, *J. Am. Chem. Soc.* **2004**, *126*, 12740.
[269] S. K. Volkman, S. Molesa, B. Matis, P. C. Chang, V. Subramanian, *Mater. Res. Soc. Symp. Proc.* **2003**, *771*, 391.
[270] H. Uno, Y. Yamashita, M. Kikuchi, H. Watanabe, H. Yamada, T. Okujima, T. Ogawa, N. Ono, *Tetrahedron Lett.* **2005**, *46*, 1981.
[271] H. Yamada, Y. Yamashita, M. Kikuchi, H. Watanabe, T. Okujima, H. Uno, T. Ogawa, K. Ohara, N. Ono, *Chem. Eur. J.* **2005**, *11*, 6212.
[272] C. F. H. Allen, A. Bell, *J. Am. Chem. Soc.* **1942**, *64*, 1253.
[273] a) N. Vets, M. Smet, W. Dehaen, *Synlett* **2005**, 217; b) N. Vets, H. Diliën, S. Toppet, W. Dehaen, *Synlett* **2006**, 1359.
[274] a) L. C. Picciolo, H. Murata, Z. H. Kafafi, *Appl. Phys. Lett.* **2001**, *78*, 2378; b) M. A. Wolak, B.-B. Jang, L. C. Palilis, Z. Kafafi, *J. Phys. Chem. B* **2004**, *108*, 5492; c) E.-J. Hwang, Y.-E. Kim, C.-J. Lee, J.-W. Park, *Thin Solid Films* **2006**, *499*, 185; d) B.-B. Jang, S.-H. Lee, Z. H. Kafafi, *Chem. Mater.* **2006**, *18*, 449; e) L. C. Picciolo, H. Murata, A. Gondarenko, T. Noda, Y. Shirota, D. L. Eaton, J. E. Anthony, Z. H. Kafafi, *Proc. SPIE-Int. Soc. Opt. Eng.* **2002**, *4464*, 383.
[275] N. Vets, M. Smet, W. Dehaen, *Synlett* **2005**, 217.
[276] Q. Miao, X. Chi, S. Xiao, R. Zeis, M. Lefenfeld, T. Siegrist, M. L. Steigerwald, C. J. Nuckolls, *J. Am. Chem. Soc.* **2006**, *128*, 1340.
[277] H. Meng, M. Bendikov, G. Mitchell, R. Helgeson, F. Wudl, Z. Bao, T. Siegrist, C. Kloc, C.-H. Chen, *Adv. Mater.* **2003**, *15*, 1090.
[278] S. H. Chan, H. K. Lee, Y. M. Wang, N. Y. Fu, X. M. Chen, Z. W. Cai, H. N. C. Wong, *Chem. Commun.* **2005**, 66.
[279] T. Takahashi, M. Kitamura, B. Shen, K. Nakajima, *J. Am. Chem. Soc.* **2000**, *122*, 12876.
[280] D. F. Perepichka, M. Bendikov, H. Meng, F. Wudl, *J. Am. Chem. Soc.* **2003**, *125*, 10190.
[281] a) Y. Sakamoto, T. Suzuki, M. Kobayashi, Y. Gao, Y. Fukai, Y. Inoue, F. Sato, S. Tokito, *J. Am. Chem. Soc.* **2004**, *126*, 8138; b) Y. Inoue, Y. Sakamoto, T. Suzuki, M. Kobayashi, Y. Gao, S. Tokito, *Jpn. J. Appl. Phys.* **2005**, *44*, 3663.
[282] P.-M. Allemand, A. Koch, F. Wudl, Y. Rubin, F. Diederich, M. M. Alvarez, S. J. Anz, R. L. Whetten, *J. Am. Chem. Soc.* **1991**, *113*, 1051.
[283] Y. Sakamoto, T. Suzuki, M. Kobayashi, Y. Gao, Y. Inoue, S. Tokito, *Mol. Cryst. Liq. Cryst.* **2006**, *444*, 225.
[284] A. R. Wartini, H. A. Staab, F. A. Neugebauer, *Eur. J. Org. Chem.* **1998**, 1161.
[285] G. S. Tulevski, Q. Miao, A. Afzali, T. O. Graham, C. R. Kagan, C. Nuckolls, *J. Am. Chem. Soc.* **2006**, *128*, 1788.
[286] K. Kobayashi, R. Shimaoka, M. Kawahata, M. Yamanaka, K. Yamaguchi, *Org. Lett.* **2006**, *8*, 2385.
[287] E. P. Goodings, D. A. Mitchard, G. Owen, *J. Chem. Soc. Perkin Trans. 1* **1972**, 1310.
[288] A. L. Briseno, Q. Miao, M.-M. Ling, C. Reese, H. Meng, Z. Bao, F. Wudl, *J. Am. Chem. Soc.* **2006**, *128*, 15576.
[289] a) M. M. Rauhut, B. G. Roberts, D. R. Maulding, W. Bergmark, R. Coleman, *J. Org. Chem.* **1975**, *40*, 330; b) P. J. Hanhela, D. B. Paul, *Aust. J. Chem.* **1981**, *34*, 1710; c) D. R. Maulding, B. G. Roberts, *J. Org. Chem.* **1969**, *34*, 1734.
[290] G. P. Miller, J. Mack, J. Briggs, *Proc. Electrochem. Soc.* **2001**, *11*, 2001.
[291] R. Schmidt, S. Göttling, D. Leusser, D. Stalke, A.-M. Krause, F. Würthner, *J. Mater. Chem.* **2006**, *16*, 3708.
[292] Y. Li, Y. Wu, P. Liu, Z. Prostran, S. Gardner, B. S. Ong, *Chem. Mater.* **2007**, *19*, 418.
[293] A. Maliakal, K. Raghavachari, H. E. Katz, E. Chandross, T. Siegrist, *Chem. Mater.* **2004**, *16*, 4980.
[294] P. Coppo, S. G. Yeates, *Adv. Mater.* **2005**, *17*, 3001.
[295] a) J. E. Anthony, J. S. Brooks, D. L. Eaton, S. R. Parkin, *J. Am. Chem. Soc.* **2001**, *123*, 9482; b) J. E. Anthony, D. L. Eaton, S. R. Parkin, *Org. Lett.* **2001**, *3*, 15.
[296] C. D. Sheraw, T. N. Jackson, D. L. Eaton, J. E. Anthony, *Adv. Mater.* **2003**, *15*, 2009.
[297] S. K. Park, T. N. Jackson, J. E. Anthony, D. A. Mourey, *Appl. Phys. Lett.* **2007**, *91*, 063514.
[298] D. H. Kim, D. Y. Lee, H. S. Lee, W. H. Lee, Y. H. Kim, J. I. Han, K. Cho, *Adv. Mater.* **2007**, *19*, 678.
[299] M. T. Lloyd, A. C. Mayer, A. S. Tayi, A. M. Bowen, T. G. Kasen, D. J. Herman, D. A. Mourey, J. E. Anthony, G. G. Malliaras, *Org. Electron.* **2006**, *7*, 243.
[300] D. C. Martin, J. H. Chen, J. Y. Yang, L. F. Drummy, C. J. Kubel, *J. Polym. Sci. Part B* **2005**, *43*, 1749.
[301] a) F. A. Hegmann, R. R. Tykwinski, K. P. H. Lui, J. E. Bullock, J. E. Anthony, *Phys. Rev. Lett.* **2002**, *89*, 227403; b) O. Ostroverkhova, D. G. Cooke, S. Scherbyna, R. Egerton, R. R. Tykwinski, J. E. Anthony, F. A. Hegmann, *Phys. Rev. B* **2005**, *71*, 035204.
[302] a) O. Ostroverkhova, S. Scherbyna, D. G. Cooke, R. F. Egerton, F. A. Hegmann, R. R. Tykwinski, S. R. Parkin, J. E. Anthony, *Phys. Rev. B* **2005**, *98*, 033701; b) O. Ostroverkhova, D. G. Cooke, F. A. Hegmann, J. E. Anthony, V. Podzorov, M. E. Gershenson, O. D. Jurchescu, T. T. M. Palstra, *Appl. Phys. Lett.* **2006**, *88*, 162101.
[303] R. C. Haddon, X. Chi, M. E. Itkis, J. E. Anthony, D. L. Eaton, T. Siegrist, C. C. Mattheus, T. T. M. Palstra, *J. Phys. Chem. B* **2002**, *106*, 8288.
[304] A. Troisi, G. Orlandi, J. E. Anthony, *Chem. Mater.* **2005**, *17*, 5024.
[305] T. Tokumoto, J. S. Brooks, R. Clinite, X. Wei, J. E. Anthony, D. L. Eaton, S. R. Parkin, *J. Appl. Phys.* **2002**, *92*, 5208.
[306] J. S. Brooks, T. Tokumoto, E.-S. Choi, D. Graf, N. Biskup, D. L. Eaton, J. E. Anthony, S. A. Odom, *J. Appl. Phys.* **2004**, *96*, 3312.
[307] D. Zhao, T. M. Swager, *Macromolecules* **2005**, *38*, 9377.
[308] Y. Kim, T. M. Swager, *Macromolecules* **2006**, *39*, 5177.
[309] Y. Kim, J. Whitten, T. M. Swager, *J. Am. Chem. Soc.* **2005**, *127*, 12122.

[310] J. E. Anthony, C. R. Swartz, C. A. Landis, S. R. Parkin, *Proc. SPIE-Int. Soc. Opt. Eng.* **2005**, *5940*, 2.
[311] a) J. Jiang, B. R. Kaafarani, D. C. Neckers, *J. Org. Chem.* **2006**, *71*, 2155; b) J. Jiang, PhD Dissertation, Center for Photochemical Sciences, Bowling Green State University, May, **2006**.
[312] M. M. Payne, J. H. Delcamp, S. R. Parkin, J. E. Anthony, *Org. Lett.* **2004**, *6*, 1609.
[313] a) M. A. Wolak, J. S. Melinger, P. A. Lane, L. C. Palilis, C. A. Landis, J. Delcamp, J. E. Anthony, Z. H. Kafafi, *J. Phys. Chem. B* **2006**, *110*, 7928; b) M. A. Wolak, J. S. Melinger, P. A. Lane, L. C. Palilis, C. A. Landis, J. E. Anthony, Z. H. Kafafi, *J. Phys. Chem. B* **2006**, *110*, 10606.
[314] M. A. Wolak, J. Delcamp, C. A. Landis, P. A. Lane, J. E. Anthony, Z. H. Kafafi, *Adv. Funct. Mater.* **2006**, *16*, 1943.
[315] C. L. Chiang, M.-F. Wu, C.-C. Dai, Y.-S. When, J.-K. Wang, C.-T. Chen, *Adv. Funct. Mater.* **2005**, *15*, 231.
[316] C. R. Swartz, S. R. Parkin, J. E. Bullock, J. E. Anthony, A. C. Mayer, G. G. Malliaras, *Org. Lett.* **2005**, *7*, 3163.
[317] R. W. Kramer, E. B. Kujawinski, P. G. Hatcher, *Environ. Sci. Technol.* **2004**, *38*, 3387.
[318] a) A. L. Mattioda, D. M. Hudgins, L. J. Allamandola, *Astrophys. J.* **2005**, *629*, 1188; b) J. L. Weisman, A. Mattioda, T. J. Lee, D. M. Hudgins, L. J. Allamandola, C. W. Bauschlicher, M. Head-Gordon, *Phys. Chem. Chem. Phys.* **2005**, *7*, 109; c) D. L. Kokkin, T. W. Schmidt, *J. Phys. Chem. A* **2006**, *110*, 6173.
[319] M. Bendikov, H. M. Duong, K. Starkey, K. N. Houk, E. A. Carter, F. Wudl, *J. Am. Chem. Soc.* **2004**, *126*, 7416; this article was corrected in M. Bendikov, H. M. Duong, K. Starkey, K. N. Houk, E. A. Carter, F. Wudl, *J. Am. Chem. Soc.* **2004**, *126*, 10493.
[320] S. Kivelson, O. L. Chapman, *Phys. Rev. B* **1983**, *28*, 7236.
[321] M. Kertesz, Y. S. Lee, J. J. P. Stewart, *Int. J. Quantum Chem.* **1989**, *35*, 305.
[322] a) C. Marschalk, *Bull. Soc. Chim. Fr.* **1939**, *6*, 1112; b) E. Clar, *Ber. Dtsch. Chem. Ges. B* **1939**, *72*, 2137; c) W. J. Bailey, C.-W. Liao, *J. Am. Chem. Soc.* **1955**, *77*, 992.
[323] M. P. Satchell, B. E. Stacey, *J. Chem. Soc. C* **1971**, 468.
[324] R. B. Campbell, J. M. Robertson, J. Trotter, *Acta Crystallogr.* **1962**, *15*, 289.
[325] H. Angliker, E. Rommel, J. Wirz, *Chem. Phys. Lett.* **1982**, *87*, 208.
[326] T. Minakata, H. Imai, M. Ozaki, *Polym. Adv. Technol.* **1995**, *6*, 602.
[327] T. Minakata, M. Ozaki, H. Imai, *J. Appl. Phys.* **1993**, *74*, 1079.
[328] E. Clar, *Ber. Dtsch. Chem. Ges. B* **1942**, *75*, 1330.
[329] C. Marschalk, *Bull. Soc. Chim. Fr.* **1943**, *10*, 511.
[330] W. J. Bailey, C.-W. Liao, *J. Am. Chem. Soc.* **1955**, *77*, 992.
[331] For an excellent overview of the controversy surrounding the synthesis of heptacene, see reference [33].
[332] R. Mondal, B. K. Shah, D. C. Neckers, *J. Am. Chem. Soc.* **2006**, *128*, 9612.
[333] a) R. Mondal, B. K. Shah, D. C. Neckers, *J. Org. Chem.* **2006**, *71*, 4085; b) J. Luo, H. Hart, *J. Org. Chem.* **1987**, *52*, 4833.
[334] a) J. B. Briggs, G. P. Miller, *C. R. Chim.* **2006**, *9*, 916; b) G. P. Miller, J. Briggs, *Org. Lett.* **2003**, *5*, 4203.
[335] a) A. D. Thomas, L. L. Miller, *J. Org. Chem.* **1986**, *51*, 4160,4169; b) S. F. Rak, T. H. Jozefiak, L. L. Miller, *J. Org. Chem.* **1990**, *55*, 4794; c) T. Chiba, P. W. Kenny, L. L. Miller, *J. Org. Chem.* **1987**, *52*, 4327; d) J. Luo, H. Hart, *J. Org. Chem.* **1988**, *53*, 1341.
[336] V. R. Sastri, R. Schulman, D. C. Roberts, *Macromolecules* **1982**, *15*, 939.
[337] M. M. Payne, S. R. Parkin, J. E. Anthony, *J. Am. Chem. Soc.* **2005**, *127*, 8028.
[338] M. M. Payne, PhD Dissertation, University of Kentucky, May **2005**.
[339] K. E. Kob, *J. Chem. Educ.* **1989**, *66*, 955.
[340] V. S. Iyer, M. Wehmeier, J. D. Brand, M. A. Keegstra, K. Müllen, *Angew. Chem.* **1997**, *109*, 1675; *Angew. Chem. Int. Ed. Engl.* **1997**, *36*, 1604.
[341] M. M. Payne, S. A. Odom, S. R. Parkin, J. E. Anthony, *Org. Lett.* **2004**, *6*, 3325.
[342] F. Würthner, R. Schmidt, *ChemPhysChem* **2006**, *7*, 793.
[343] V. Schomaker, K. N. Trueblood, *Acta Crystallogr. Sect. B* **1968**, *24*, 63.
[344] C. A. Landis, S. R. Parkin, J. E. Anthony, *Jpn. J. Appl. Phys.* **2005**, *44*, 3921.
[345] a) T. M. Krygowski, M. K. Cyranski, *Chem. Rev.* **2001**, *101*, 1385; b) P. Bultinck, M. Rafat, R. Ponec, B. Van Gheluwe, R. Carbó-Dorca, P. Popelier, *J. Phys. Chem. A* **2006**, *110*, 7642.
[346] K. N. Houk, P. S. Lee, M. Nendel, *J. Org. Chem.* **2001**, *66*, 5517.
[347] E. S. Kadantsev, M. J. Stott, A. Rubio, *J. Chem. Phys.* **2006**, *124*, 134901.
[348] *Electronic Materials: The Oligomer Approach* (Eds.: K. Müllen, G. Wegner), Wiley-VCH, Weinheim, **1998**.
[349] S. Haas, A. F. Stassen, G. Schuck, K. P. Pernstich, D. J. Gundlach, B. Batlogg, U. Berens, H.-J. Kirner, *Phys. Rev. B* **2007**, *76*, 115203.
[350] C. P. Benard, Z. Geng, M. A. Heuft, K. VanCrey, A. G. Fallis, *J. Org. Chem.* **2007**, *72*, 7229.
[351] T. Okamoto, Z. Bao, *J. Am. Chem. Soc.* **2007**, *129*, 10308.
[352] D. Lehnherr, R. R. Tykwinski, *Org. Lett.* **2007**, *9*, 4583.
[353] M. Winkler, K. N. Houk, *J. Am. Chem. Soc.* **2007**, *129*, 1805.
[354] M.-Y. Kuo, H.-Y. Chen, I. Chao, *Chem. Eur. J.* **2007**, *13*, 4750.
[355] R. Mondal, R. M. Adhikari, B. K. Shah, D. C. Neckers, *Org. Lett.* **2007**, *9*, 2505.